ELSEVIER

Journal of Structural Geology 29 (2007) 712–735

JOURNAL OF STRUCTURAL GEOLOGY

www.elsevier.com/locate/jsg

Fault and vein relationships in a reverse fault system at the Centenary orebody (Darlot gold deposit), Western Australia: Implications for gold mineralisation

Shane Kenworthy*, Steffen G. Hagemann

School of Earth and Geographical Sciences, The University of Western Australia, 35 Stirling Highway, Crawley, Western Australia 6009, Australia

Received 7 October 2005; received in revised form 22 October 2006; accepted 18 November 2006
Available online 16 January 2007

Abstract

The Centenary orebody within the Darlot gold deposit is located in the Yandal greenstone belt in the Yilgarn Craton, Western Australia. At Centenary, moderately (~45°) west dipping reverse faults and steeply dipping (>70°) faults of variable strike failed during gold mineralisation in response to sub-horizontal east-west shortening and sub-vertical extension. Gently dipping veins are temporally, genetically and spatially related subsidiary structures to west dipping reverse and steeply dipping faults. Line analyses of subsidiary vein distributions in 23 drill cores around Centenary suggest that the gold-related subsidiary veins are localised within a 200–300 m wide tabular linking damage zone between three west dipping faults (Thompson, Lords and Walters). The damage zone is a laterally stepping relay zone between the Thompson and Lords–Walters faults and has a pull-apart geometry. Anomalous vein-related extensional strain (>0.005), vein density (>0.20) and power-law vein thickness population characteristics (D_t 0.58–1.84) distinguish this zone from the surrounding rock.

Within the linking damage zone the highest number and volume of veins are observed at the tip of the Walters fault. At the fault tip, the exponent of the power-law distribution of vein thickness is highest (D_t 1.84) indicating that vein-related extensional strain is distributed on a high number of relatively small thickness veins. At approximately 300 m distance from the fault tip the densities of veins and the measured exponents of power-law vein thickness distributions are lower (<0.80 and D_t <1.3, respectively). However, bulk vertical extensional strain remains high (>0.005), indicating that subsidiary vein material is concentrated on a greater number of anomalously thick veins. These systematic variations suggest that the fault tip imparted a strong control on vein localisation. Strain localisation within the linking damage zone is complex with coefficients of variation of vein spacing greater than one implying vein clustering. Gently dipping veins occur as wing crack arrays to the reverse faults and also in arrays comprising curviplanar, intersecting networks of subsidiary veins. The linking damage zone corresponds closely with the Centenary gold resource indicating that it has been an important locus for the focussed flux of gold-bearing hydrothermal fluids. However, within the damage zone, individual veins and vein arrays on the tens of metre scale do not always correlate with high gold grade indicating additional complexity within the system.

Keywords: Damage zone; Vein distribution; Extensional strain; Fault zone; Fluid; Gold

1. Introduction

Structural focussing of gold-bearing hydrothermal fluids is critical to the formation of orogenic lode gold deposits hosted in granite and volcanosedimentary terranes (Groves et al., 1995; Hagemann and Cassidy, 2000). Domains comprising a high density of interconnected structures are potential sites of high palaeo-fluid flux and hence may be of economic significance (cf. Cox et al., 2001). Many brittle-(ductile) faults are enveloped by a damage zone of strained rock in which there is an elevated level of subsidiary structures such as fractures and minor extent and displacement faults (Chester and Logan, 1986; Evans et al., 1997). Damage zones at fault heterogeneities such as restraining and releasing bends, relay zones and

* Corresponding author. Tel.: +61 8 6488 7147; fax: +61 8 6488 1178.
E-mail address: shane_kenworthy@yahoo.com (S. Kenworthy).

0191-8141/$ - see front matter © 2006 Elsevier Ltd. All rights reserved.
doi:10.1016/j.jsg.2006.11.004

fault tips can be particularly well-endowed in those subsidiary structures (McGrath and Davison, 1995; Kim et al., 2003; Kim et al., 2004). These sites can host epigenetic, hydrothermal mineralization and are, therefore, of interest to explorationists (cf. Gillerman, 1988; Kennworthy et al., 2001).

In this paper, we present a detailed documentation and interpretation of internal structures of a linking damage zone between three moderately dipping reverse-(oblique) faults at the Centenary orebody in Western Australia. The damage zone comprises metre to tens of metre length, gently dipping veins within a 200–300 m wide zone between three major faults. The relationship between the faults and veins is evaluated by the integration of detailed underground mine structural maps with line analysis of vein distributions in diamond drill core. First, we document the geometry, kinematics, spatial distributions and internal structures and textures of the major faults. Second, the geometry, internal structures and textures of metre scale veins are presented and their spatial distribution and thickness in drill cores around Centenary are examined. Data-sets of the faults and metre scale veins are integrated into a semi-quantitative structural model, which highlights systematic variations in the distribution and properties of veins along and around the faults. The structural model has implications for the genesis of the faults and metre scale veins as well as for the localisation of fluid flux and gold mineralisation.

2. Regional geology

The Centenary orebody is part of the Archaean Darlot gold deposit, located at the southern part of the Yandal greenstone belt in the Yilgarn Craton, Western Australia. The Yandal greenstone belt comprises a 220 km long, up to 40 km wide north-northwest trending Archaean volcanosedimentary greenstone succession, bounded by Archaean granitoid-gneiss terranes (Fig. 1). Metamorphic grade reaches amphibolite facies at the margins of the belt, whereas rocks in the rest of the belt typically preserve greenschist facies (Westaway and Wyche, 1998). Primary textures are generally well preserved and original rock types can be identified, so the prefix meta- is assumed but omitted in the following discussion. Narrow sequences of chert and banded iron formation occur at the northwest margin of the greenstone belt and calc-alkaline intrusive, extrusive and volcaniclastic rocks of the Spring Well Sequence occur in the south of the greenstone belt (Giles, 1982; Phillips et al., 1998; Messenger, 2000). Mafic extrusive and intrusive rocks with some dacitic volcanic and sedimentary rocks dominate the rest of the greenstone belt (Phillips et al., 1998; Messenger, 2000).

The earliest recognised deformation in the belt includes gentle south dipping thrusts, north-verging recumbent folds and high strain zones that contain a foliation which is parallel to bedding and igneous layering in the greenstone belt (Chen et al., 2001). High strain zones are folded about prominent north- to northwest trending upright folds that are accompanied by axial planar foliations (Westaway and Wyche, 1998; Chen et al., 2001). Locally, the north to northwest trending folds are truncated by north-northeast to northwest trending regional shear zones (Westaway and Wyche, 1998). Dextral faults trending 040–060° and sinistral faults trending 090–120°, crosscut the greenstone belt and regional shear zones (Vearncombe, 1998). Numerous Archaean granitoid, porphyry and lamprophyre stocks and dykes occur within the belt (Westaway and Wyche, 1998), as well as east- and east-southeast striking Proterozoic dolerite dykes (Phillips et al., 1998; Messenger, 2000). Archaean lode gold mineralisation occurs throughout the greenstone belt at deposits such as Jundee-Nimary (168 t Au), Bronzewing (73 t Au), Mount McClure (55 t Au) and Darlot (85 t Au; Fig. 1; Beardsmore and Gardner, 2003; Kohler and Phillips, 2003; Kohler et al., 2003; Phillips and Vearncombe, 2003).

3. Local geology

The Centenary orebody is one of two spatially distinct gold-quartz vein orebodies that comprise the Darlot gold deposit, the other is the Darlot orebody (Fig. 2). The structurally lowest and stratigraphically oldest rocks at the Darlot deposit occur to the west of the Centenary orebody and comprise mafic and felsic volcanic and minor sedimentary rocks (Fig. 2; Krcmarov et al., 2000). To the east, at the Centenary orebody, the volcanosedimentary rocks are intruded by the Mount Pickering dolerite sill. Zones of intrusive breccia are observed at the base, and locally in the central portions of the sill and comprise enclaves of felsic and mafic volcanic rocks in a matrix of the Mount Pickering dolerite. The Mount Pickering dolerite has been divided into seven units on the basis of mineralogical and textural variations (Krcmarov et al., 2000; Beardsmore and Gardner, 2003). From the base to the top of the sill these are lower porphyritic dolerite, lower leucodolerite, mesocratic dolerite, magnetite (± quartz) dolerite, upper leucogabbro, upper porphyritic dolerite and marginal dolerite. Most of the Centenary orebody is hosted within the magnetite (± quartz) dolerite with minor portions in the mesocratic dolerite and upper leucogabbro units of the sill (Beardsmore and Gardner, 2003). The Mount Pickering dolerite is overlain by mafic and felsic volcanic rocks and minor sedimentary rocks. Volcanosedimentary rocks and the Mount Pickering dolerite have undergone regional greenschist facies metamorphism. Dykes and intrusive bodies of lamprophyric affinity in association with granitoid are observed at the deposit.

The structural, magmatic and hydrothermal evolution of the Darlot deposit, as presented below, is summarised in Table 1. Supracrustal rocks at Darlot are folded about the gentle northwest plunging, upright open Darlot syncline (Fig. 2). This fold belongs to the earliest recognised deformation event at the deposit and is not accompanied by a widespread foliation. The northwest striking, moderately (50–65°) northeast dipping El Dorado shear zone truncates and offsets the southwest limb of the Darlot syncline, with approximately 1500 m of apparent sinistral displacement (Fig. 2). Lamprophyric intrusions cross the El Dorado shear zone but are offset less than 100 m, suggesting that lamprophyric magmatism occurred late- to post-displacement of the El Dorado shear zone.

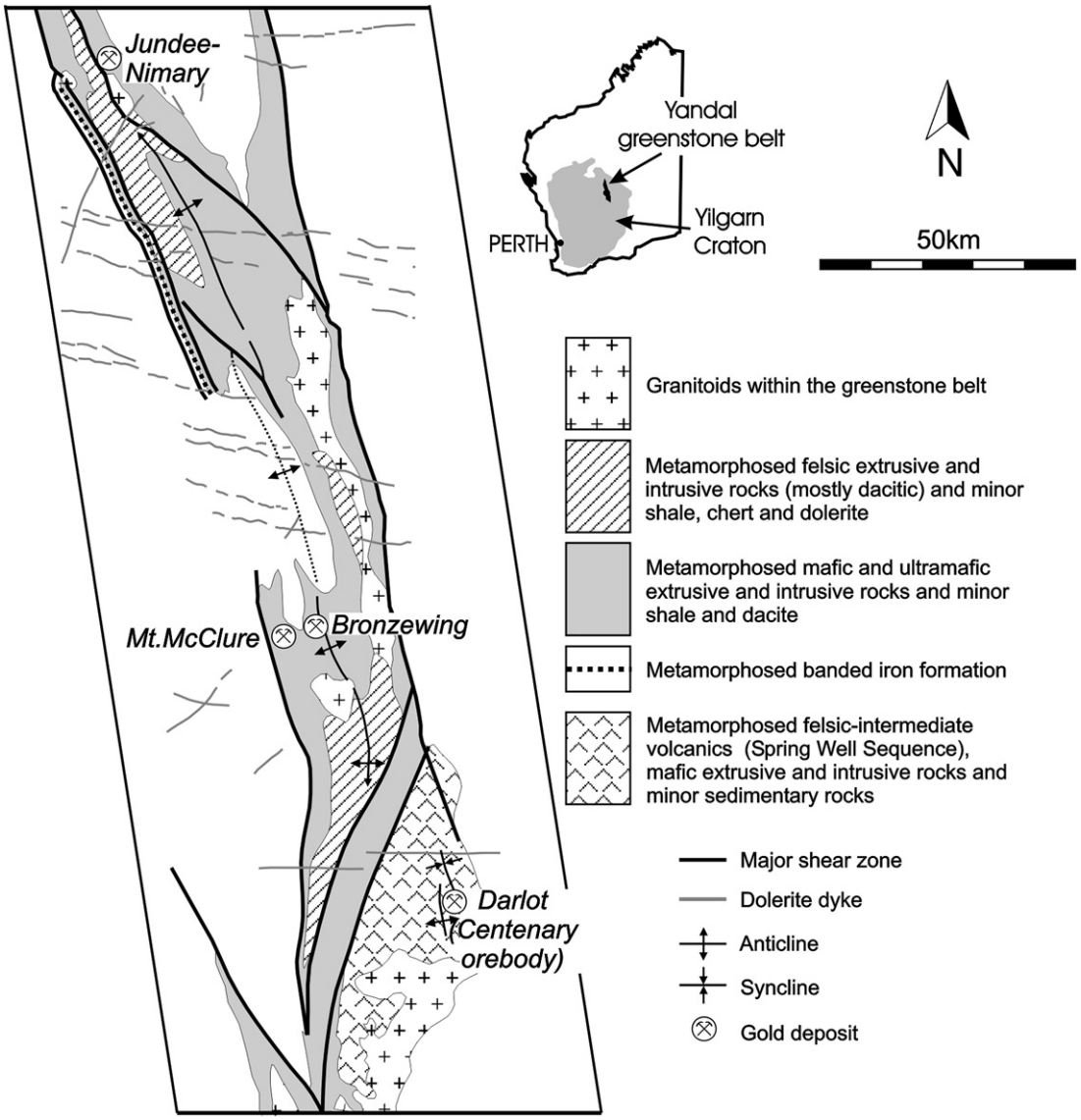

Fig. 1. Simplified geological map of the Yandal greenstone belt showing distribution of rock types, structures and locations of major gold deposits, including Darlot (modified from Messenger, 2000).

Lamprophyre dykes have multiple orientations, which have been divided into three sets. One set comprises a distinct population of east to south striking dykes that dip steeply (>70°; Fig. 3a). The second set is moderately (~45°) east and west dipping and the third set comprises rare sub-horizontal dykes. Rare, steeply dipping (>70°), east striking quartz-epidote-chlorite veins have mutually crosscutting relationships with lamprophyre dykes (Fig. 3b).

Moderately (~45–60°) east and west dipping gold-bearing reverse-(oblique) faults crosscut or are localised within lamprophyre dykes (Figs. 3c and 4). These faults have offsets of up to 100 m. Sub-horizontal to moderately dipping (45°), north striking veins fringe the reverse faults and also occur in isolated vein arrays (Figs. 3d and 5). Locally veins in the vein arrays are northeast striking and steeply dipping (>70°) and they sometimes occur along the margins of steeply dipping lamprophyre dykes (Figs. 3d and 5). Steeply dipping (>70°) predominantly northeast to east striking and, to a lesser extent, east to southeast striking faults offset and bound reverse faults and associated gently dipping veins (Fig. 3e). Apparent sinistral and dextral offsets are observed along steeply dipping faults in plan view and gently plunging (<20°) slickenlines on fault planes indicate the last recorded movement on many faults was dominantly strike-slip. However, metre scale normal and rare less than 20 cm reverse offsets are also observed on some faults that have steeply plunging (>70°) slickenlines. Locally, steeply dipping faults are gold-bearing and are fringed by gently dipping veins suggesting that at least some were active during development of the gold-bearing reverse faults (Fig. 4 photo). Reverse faults are crosscut by arrays of steeply dipping (70°), predominantly east-northeast striking quartz-carbonate-chlorite ± haematite veins, fractures and late normal and reverse faults that have offsets less than 10 cm (Fig. 3f).

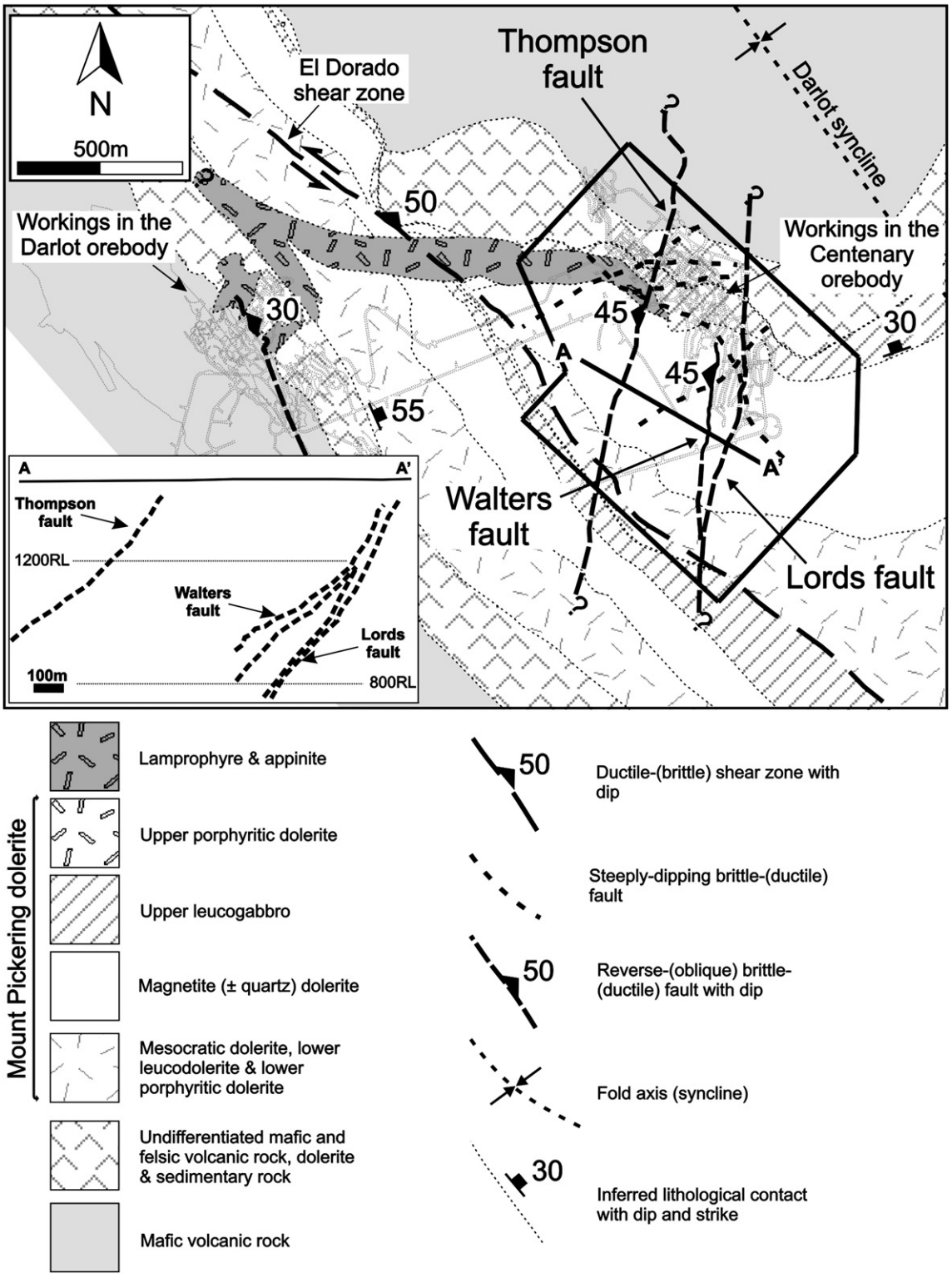

Fig. 2. Simplified interpreted geology map of the Darlot deposit at the 1080 RL (about 380 m below current surface). Area containing drill cores and underground exposures analysed at the Centenary orebody is marked. Inset shows section across the Lords and Walters faults.

4. The Centenary fault system during gold mineralisation

Gold occurs in veins and surrounding hydrothermal wall rock alteration associated with: (1) west dipping reverse faults, (2) gently dipping, subsidiary veins, and the (3) steeply dipping faults that offset and bound the reverse faults and gently dipping veins (Table 1). The gently dipping veins are subsidiary to the reverse and steeply dipping faults and at the orebody scale comprise a linking damage zone between three major west-dipping reverse faults: the Lords, Walters

Table 1
Relative timing of structural, magmatic and hydrothermal events at the Darlot deposit

	Structural-hydrothermal-dyke events	
A	Shallowly (~15°) northwest plunging, upright open Darlot syncline	Oldest
B	Fold limb offset by: northwest striking, moderately (50–65 °) northeast dipping El Dorado shear zone	
C	Lamprophyres intrude across the El Dorado shear zone with minimal offset: (i) steeply dipping (>70°), northeast to east striking and lesser east to southeast striking lamprophyre dykes; (ii) north striking, moderately (45–60°) east and west dipping lamprophyre dykes; (iii) rare sub-horizontal lamprophyre and granitoid dykes; (iv) rare, steeply dipping (>70°), east striking quartz-epidote-chlorite veins (mutually crosscutting with lamprophyres)	
D	Lamprophyre dykes are reactivated and accompanied by formation of: (i) north striking, moderately (~45–60°) east and west dipping gold-bearing reverse-(oblique) fault zones; (ii) sub-horizontal to moderately dipping (45°), north striking gold-bearing veins; (iii) steeply dipping (>70°) predominantly northeast to east striking and, to a lesser extent, east to southeast striking, locally gold-bearing fault zones	Centenary fault system
E	Gold-bearing fault zones and veins are crosscut by: steeply dipping (>70°), predominantly east-northeast striking veins, fractures and normal and reverse faults that have offsets less than 10 cm	Youngest

and Thompson (Fig. 2). Structures associated with gold mineralisation are the focus of the remainder of the paper and are discussed in two main divisions: (1) faults, and (2) subsidiary veins.

Faults at Centenary can be traced by fault-fill veins (terminology from Cox, 1995) that occupy the central portions of the reverse faults and by foliated wall rock and fault-fill veins that comprise the steeply dipping faults. The linking damage zone at Centenary is defined by the gently dipping veins that are subsidiary to the faults. Data are first presented for the faults followed by data for the subsidiary veins. A subsequent analysis of vein distributions in drill core is presented in which the properties of the subsidiary veins are evaluated in relation to the faults.

5. Description of faults and subsidiary veins

5.1. General features of reverse faults

Three important west dipping reverse faults, the Lords, Walters and Thompson, occur at Centenary (Fig. 2). The

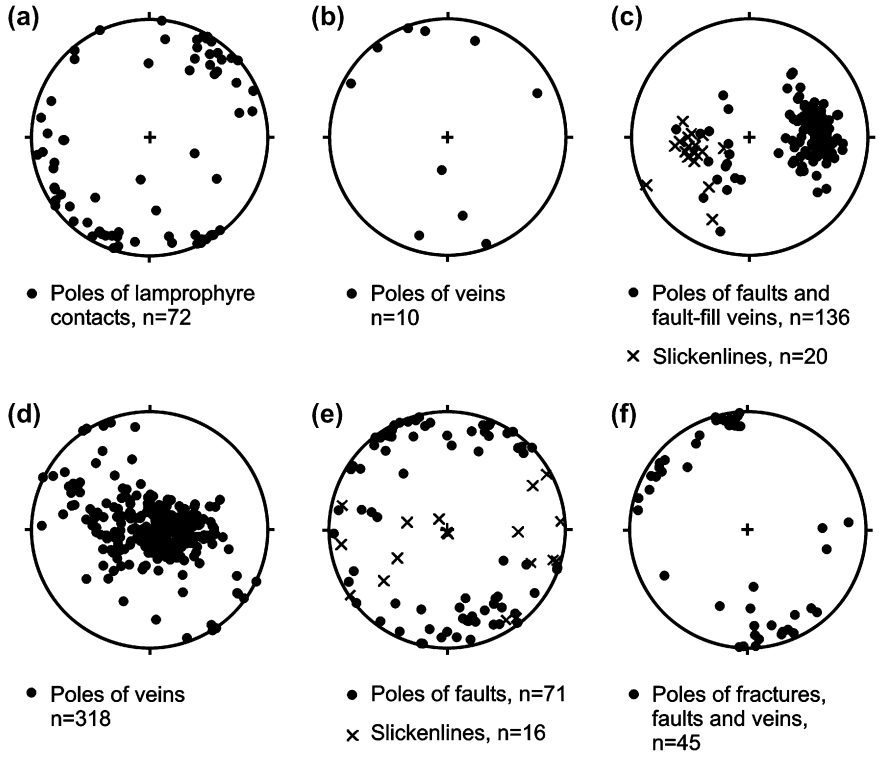

Fig. 3. Equal area, lower hemisphere projections of structural elements at Darlot. (a) Poles to lamprophyre dykes. Not included on this plot are sheared, dismembered and brecciated lamprophyre dykes that parallel moderately west-dipping faults. (b) Poles to quartz-epidote-chlorite veins that have mutually crosscutting relationships with lamprophyre dykes. (c) Poles to moderately dipping reverse-(oblique) faults and associated slickenlines. (d) Poles to veins in arrays that are coeval with moderately dipping reverse-(oblique) faults. (e) Poles to faults that crosscut and bound moderately dipping reverse-(oblique) faults. Also shown are slickenlines on these steeply dipping faults. (f) Poles to veins, fractures and faults that crosscut moderately dipping reverse-(oblique) faults.

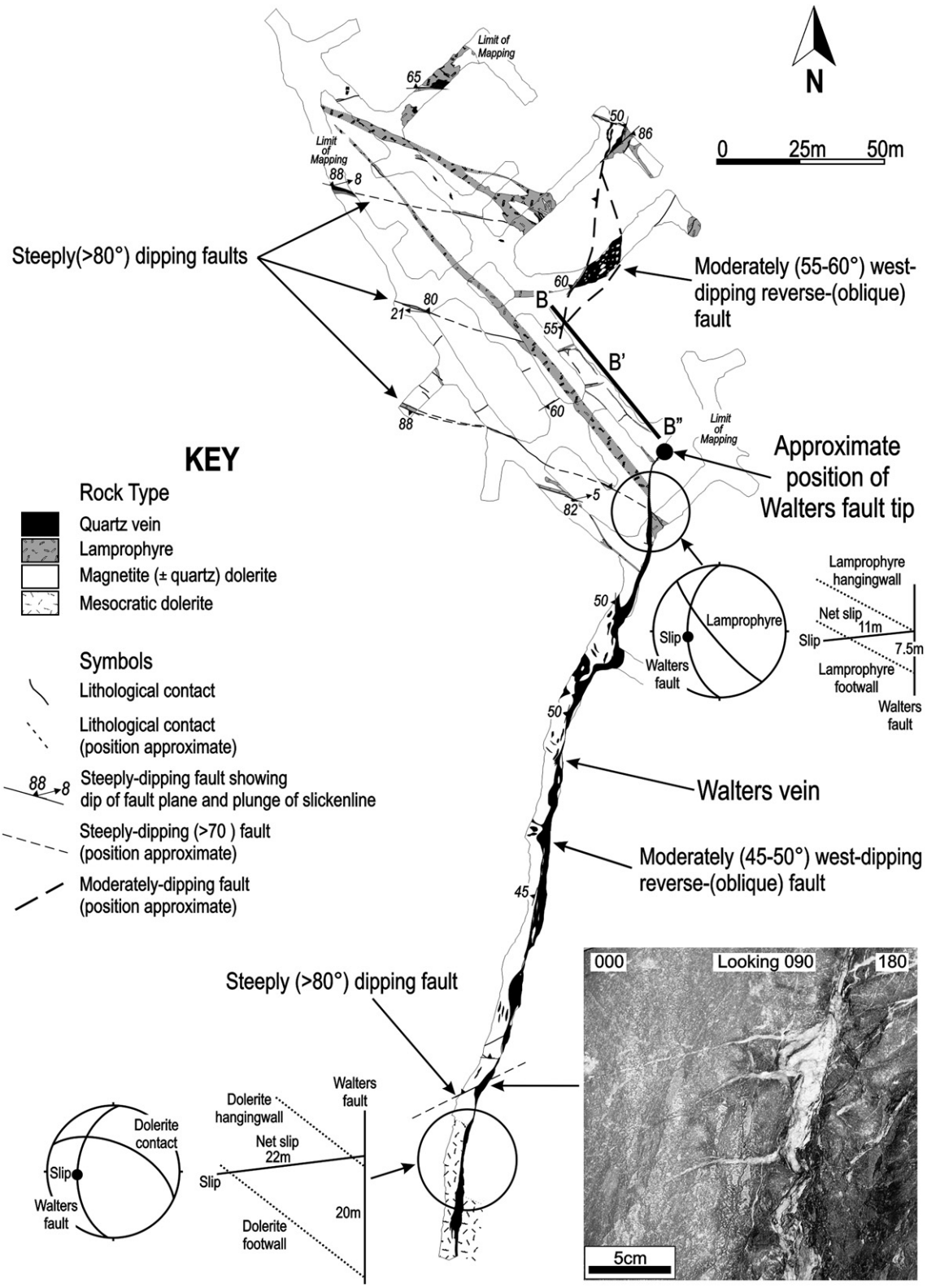

Fig. 4. Map of the 1100 level at the Centenary orebody (about 360 m below current surface) showing distribution of moderately and steeply dipping faults. Photograph shows steeply dipping fault with laminated fault-fill vein and fringing sub-horizontal veins that pinch with distance from the fault-fill vein. The two circles show a decrease in the estimated net slip along the Walters fault (22–11 m) following the method of Ragan (1985).

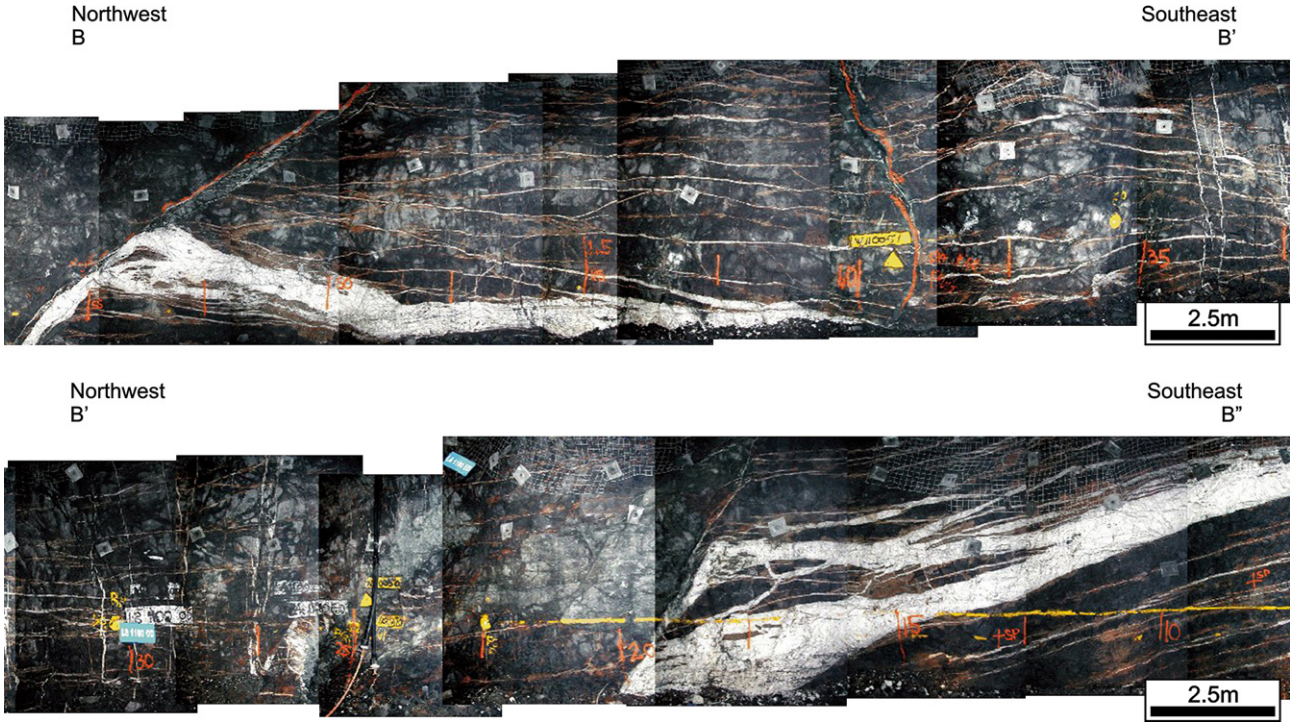

Fig. 5. Photographs showing sub-horizontal, moderately and steeply dipping veins at the 1100 level, Centenary orebody. Gently dipping veins are wing cracks to the moderately west dipping reverse faults. For location of photographs see Fig. 4.

Lords fault is located along most of its strike and dip within a 1–10 m thick lamprophyre dyke and dips about 50–65° to the west. The about 45° west dipping Walters fault merges with the Lords fault about 220 m below the present surface (Fig. 2 inset). Below 220 m the faults diverge with the more steeply dipping Lords fault in the footwall of the Walters fault (Fig. 2 inset). The two faults converge along strike to the south but the Walters fault terminates to the north. At the northern termination the Walters fault splays into a package of centimetre to metre thick gently dipping veins and left-stepping reverse faults that comprise the linking damage zone (Figs. 4 and 5). The veins illustrated in Fig. 5 occur as wing cracks to the minor faults (cf. Rispoli, 1981). The tip of the Walters fault occurs within magnetite (± quartz) dolerite of the Mount Pickering dolerite, however, in detail the fault tip most closely coincides with an irregular lamprophyric body and an intrusive breccia comprising enclaves of felsic volcanic rock within magnetite (± quartz) dolerite (Fig. 4). Offsets of rock units near the Walters fault tip are less than 5 m which is considerably less than the 20–30 m offset at the centre of the fault (Fig. 4). The about 45° west dipping Thompson fault occurs around 500 m into the hanging wall of the Walters fault (Fig. 2).

Margins and slip planes within the Walters and Lords fault-fill veins display moderately west-southwest plunging slickenlines (Fig. 3c). Fault cores vary in width from a singular slip plane, to zones in excess of 3 m width comprising fracture networks, fault parallel slip planes and a foliation which is mostly parallel to the fault but locally dips at more than 70°. Fault-fill veins are up to 7 m thick with local bifurcations both along strike and down-dip. Gently dipping subsidiary veins fringe the hanging wall and footwall of the fault-fill veins.

5.2. Internal structure and texture of fault-fill veins of reverse faults

Fault-fill veins are composed mostly of massive, milky white quartz and laminations. Laminations comprise white mica and chlorite and are concordant or slightly discordant with the vein margins and locally merge into wall rock breccia clasts (Fig. 6a). Wall rock breccia clasts are angular and of up to metre scale dimensions. Locally, laminae are styolitic with styolite peaks indicating shortening at a high angle to the vein margins. Vugs are common within the fault-fill veins and contain crystals of quartz and locally carbonate, pyrite, chalcopyrite and sphalerite (Fig. 6b). Curviplanar, intersecting, striated slip planes, some coated with galena and pyrite, separate sections of the veins (Fig. 6c). Quartz grains between laminae are either coarse and between 0.4 and 5.0 mm or recrystallised finer grains less than 0.5 mm. Most coarse-grained quartz is xenoblastic and displays moderate to strong undulose extinction, incipient subgrain development and sutured and recrystallised grain boundaries. Coarse grains of 0.4–5.0 mm size of subidioblastic carbonate and albite fringe vein margins, wall rock slivers and breccia clasts.

5.3. Distribution and geometry of fault-fill veins of reverse faults

Structural contour maps of the Lords, Walters and Thompson fault-fill veins display relatively simple planar

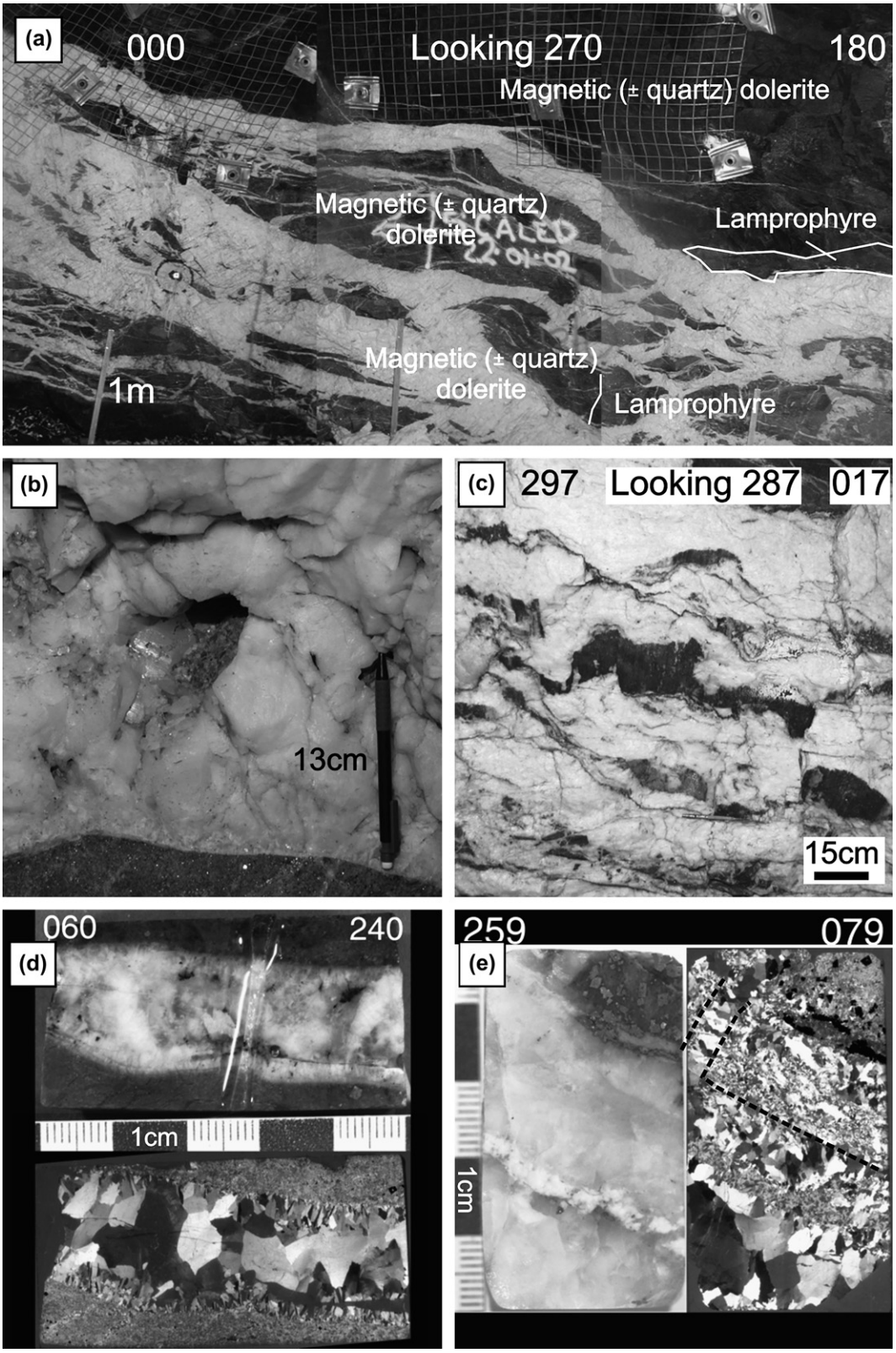

Fig. 6. Photographs showing internal structures and textures of veins at the Centenary orebody. (a) Thompson fault-fill vein containing subangular to angular magnetite (± quartz) dolerite and lamprophyre breccia clasts (1030 RL). (b) Vug in the Walters vein with prismatic quartz crystals which protrude into the open-space (1040 RL). (c) Walters fault-fill vein showing curviplanar and intersecting, galena- and pyrite-coated, striated slip planes sub-parallel to the vein margins (1100 RL). (d) Photograph of rock block and corresponding photograph of thin section under cross-polars showing aligned plagioclase crystals on vein margins and interlocking quartz crystals in vein centre (1100 RL). (e) Photograph of rock block and corresponding photograph of thin section under cross-polars showing coarse- and fine-grained quartz zones separated by relatively sharp contacts. This vein is interpreted to have formed by dilation and infilling of the southeast-dipping fracture by fine-grained quartz, which has subsequently been re-fractured, in combination with the northwest-dipping fracture and infilled by coarse quartz and carbonate (1045 RL).

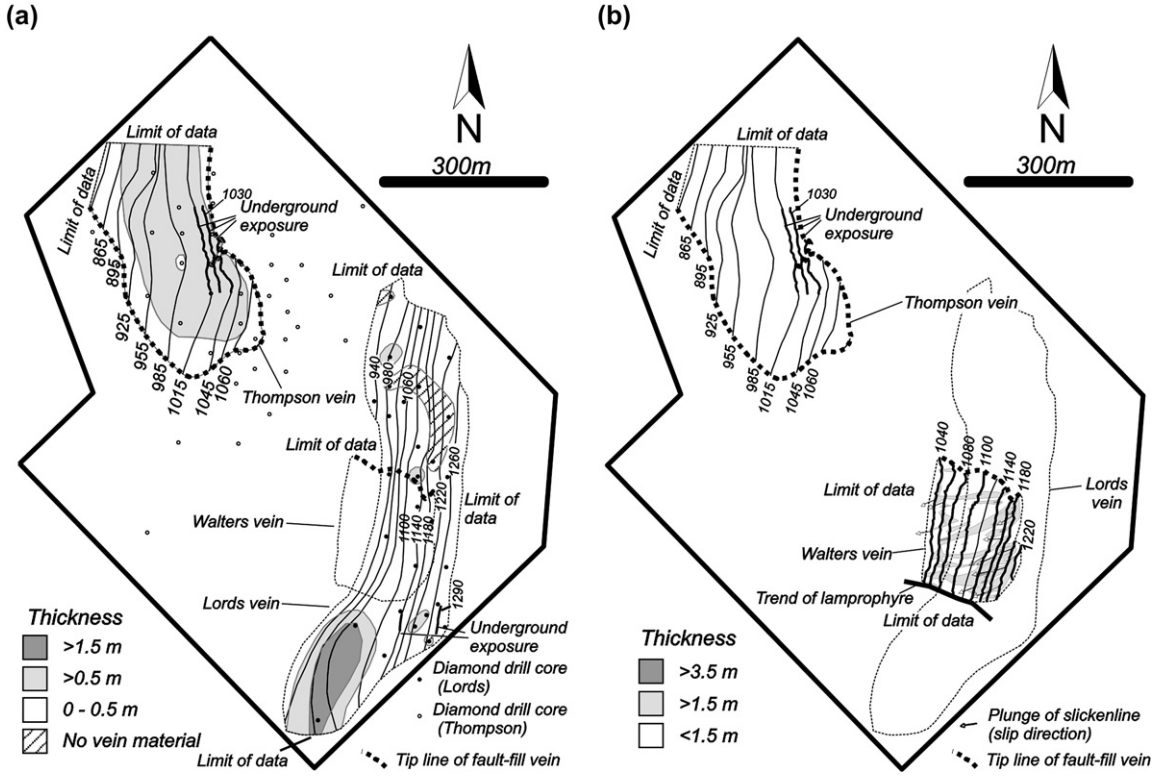

Fig. 7. Plan projections of the Lords, Walters and Thompson fault-fill veins showing structural contours. Thick borders on the diagrams correspond with the area marked on Fig. 2. (a) Lords and Thompson fault-fill veins showing vein thickness. Locations of drill cores used to construct diagram are shown. (b) Walters and Thompson fault-fill veins.

morphologies (Fig. 7). The limits of the Lords vein correspond with the data extents defined by the available drill cores (Fig. 7a). The southern limits of the Thompson vein are real as indicated by the absence of quartz vein in underground exposures. However, fault-fill veins, geometrically and spatially consistent with the Thompson fault, but unconnected to the Thompson vein suggest that the Thompson fault continues south beyond the Thompson vein (Fig. 7a). The northern extent of the Thompson vein is apparent and represents the limit of the available drill core data (Fig. 7a). The limits of the Walters vein are defined by underground mapping of exposures that extend down to the 1040 relative level (RL), which is a locally used height measurement (in metres) referenced to sea level (Fig. 7b). Structural contours for the Lords and Thompson veins are subject to a moderate degree of uncertainty due to the interpolation required of the spaced drill core data. In general, the Lords vein has a relatively regular dip, whereas the Thompson vein has a gentler dip between the 955 and 1015 RL. Structural contours for the Walters vein can be interpreted with confidence due to the detailed mapping (1:250). The Walters vein has a gentler dip between the 1140 and 1080 RL and rotates to an east-southeast strike at the vein's southern extent, following an earlier lamprophyre dyke (Fig. 7b). Little information is available regarding the Walters vein to the south of the lamprophyre dyke. The northern limit of the Walters vein occurs where the vein pinches or splays into an array of gently dipping, subsidiary veins. This termination is used as a proxy for the Walters fault tip.

Contoured vein thickness for the Lords vein suggests that a veneer of vein less than 0.5 m thick covers most of the principal displacement zone of the fault (Fig. 7a). A zone of higher vein thickness occurs at the southern end of the Lords vein between the 960 and 1100 RL coincident with the approximate location of merging of the Lords and Walters faults. Contoured vein thickness for the Thompson vein is more regular and predictable, increasing from zero at the vein margins to a maximum around the vein centre (Fig. 7a). The 0.5 m thickness limit for the Thompson vein is defined on the basis of drill core data but the vein reaches thicknesses of up to 5 m in underground exposures. Contoured vein thickness for the Walters vein suggests pipe-like segments of vein material greater than 1.5 m thick are parallel to slickenlines on the fault (Fig. 7b). No relationship is observed between the thickness of the Walters vein and intersections with steeply dipping faults.

5.4. Steeply dipping faults

Numerous steeply dipping faults are observed at the Centenary orebody that locally are sub-parallel but also interlink or splay to form a pattern with a braided appearance (Fig. 4). The steeply dipping faults have widths less than 2 m and lateral and vertical extents ranging from less than 10 m to kilometres. Steeply dipping faults contain foliated wall rock and quartz-carbonate-albite-(pyrite-haematite) fault-fill veins. Individual segments of fault-fill veins within the steeply dipping faults

have areas that are typically less than 20 m^2. Locally, fault-fill veins are laminated, brecciated and/or contain vugs.

5.5. General features of subsidiary veins

Subsidiary veins of the linking damage zone occur in a 400 m long, 200–300 m wide, up to 250 m high northwest trending zone between the Lords and Thompson faults and are well exposed by underground mine workings. Most veins dip at less than 20° but there is a pronounced group of north-striking veins that have dips up to about 45° (Fig. 3d). Fractures continue from the tips of some veins. Locally, the veins occur as wing cracks adjacent to reverse faults (Fig. 5). In other areas the veins are curviplanar in three-dimensional space, curving, branching and splaying along strike and dip and terminating in splays (Fig. 8). Locally, veins interlink to form meshes (Fig. 8). Offsets of most vein margins indicate vertical opening but some display centimetre to metre scale reverse and rare centimetre scale normal offsets. Lateral offsets of vein margins are also observed on some sub-horizontal veins. Reverse brittle-ductile fault zones, containing en echelon sigmoidal veins, have nearly horizontal to moderately dipping (~45°) trends and variable strike (Fig. 8). Locally, veins occur in the centre of the reverse brittle-ductile fault zones but given their relatively limited areas (<100 m^2), they are differentiated from fault-fill veins that fill kilometre-length faults.

5.6. Internal structure and texture of subsidiary veins

Most subsidiary veins are massive but wall rock laminations and vugs are observed locally. Most veins have interlocking crystals and lack crackseal inclusion bands or trails (Fig. 6d). Some veins have two, possibly three, different crystal morphologies separated by sharp vein margin parallel boundaries indicating several dilation and infilling events (Fig. 6e). Locally, moderately dipping and sub-horizontal veins are joined by interlocking crystals. Weak sub-vertical or vein margin perpendicular alignments of the long axes of quartz, carbonate and albite crystals are observed in some veins. Quartz is the most volumetrically significant vein fill and has a medium to coarse grain-size (0.2–12 mm). Quartz grains are xenoblastic and display moderate undulose extinction, sutured grain boundaries, minor recrystallisation and subgrain development. Carbonate and albite fringe vein margins and rarely define median lines within the centre of veins (Fig. 6d). Pyrite is observed as subidioblastic to idioblastic cubes occurring in the central portions of veins or crossing from wall rock into vein. Chlorite and white mica occur as radiating or massive aggregates within the central portions of veins or centimetre scale dilatational jogs.

6. Analysis of vein distributions

6.1. Analytical techniques and conventions

Measurements of veins in drill core were used to characterise gold-associated veins at Centenary. The apparent thickness, true thickness, angle to vertical and spacing were measured for all veins intersected on lines down the centre of surfaces of sub-vertically orientated half drill core. Vein mineralogy and texture were also recorded. Twenty-one drill cores were examined, varying in length from 232 to 529 m and totalling 8420 m (Table 2). Gold-associated, quartz ± carbonate ± albite veins with dips less than 45° and massive or open space-filling textures were measured. Many veins are enveloped by hydrothermal alteration associated with gold mineralisation. As an arbitrary lower limit, only veins greater than 5 mm were measured. Although veins with thickness below 5 mm may help to elucidate the initial fracture density of the rock mass, this is not the focus of the paper and these finer veins do not impact on the overall conclusions. Measurements were taken to the nearest millimetre and the core was orientated to obtain a true width measurement. Veins belonging to hydrothermal and deformation events that pre- and post-date gold-associated veins were not recorded. Veins not associated with gold mineralisation are relatively minor and can be distinguished by their mineralogy, internal structures and textures, geometry and associated hydrothermal alteration (e.g. post-gold, sub-vertical quartz-carbonate-chlorite ± haematite veins).

6.2. Vertical extensional strain

The reverse faults and the open-space filling textures of gently dipping, subsidiary veins are consistent with failure due to progressive sub-horizontal east-west shortening and sub-vertical extension. Assuming the subsidiary veins

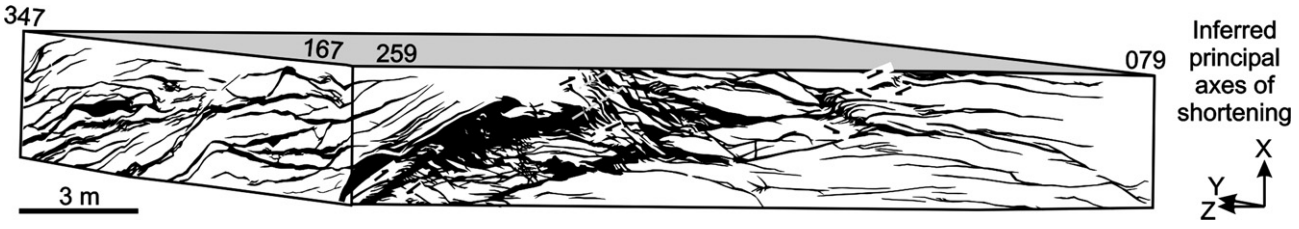

Fig. 8. Block model of a vein array in the footwall of the Thompson fault-fill vein (1045 RL). The east-striking section displays less than 45° dipping en echelon arrays of sigmoidal veins within brittle-ductile reverse fault zones. Veins in the centre of the east-striking section are rotated about 45° west-dipping reverse fault zones. Vein geometries vary along strike and dip and veins interlink to form a mesh. Kinematics of structures suggests sub-horizontal east-west shortening and vertical extension.

Table 2
Summary of vein distributions in drill cores about the Centenary orebody

HoleId	Mean	Mode	SD	Range	Min	Max	*N*	Sum (all)	Sum (sub)	L_f (m)	*e* (sub)	*d* (vein/m)	CFT	Lin. Int.	*r*	D_t	C_v
MCD0401	29.32	5	93	914	5	919	99	2903	2903	449.93	0.006	0.22	CU				1.82
MCD0402	30.75	5	28	103	5	108	16	492	492	331.20	0.001	0.05	P	5 to 45	0.96	0.58	1.53
MCD0413	24.80	5	18	53	5	58	15	372	372	357.50	0.001	0.04	P	5 to 28	0.96	0.59	0.87
MCD0426	50.38	5	141	907	5	912	86	4333	3421	437.80	0.008	0.20	P		0.99	0.87	2.02
MCD0431	55.38	9	120	706	5	711	77	4264	3553	529.00	0.007	0.15	P*	5 to 188	0.99	0.68	2.52
MCD0432	24.18	5	91	850	5	855	88	2128	1273	498.40	0.003	0.18	P*	5 to 53	0.99	1.39	1.48
MCD0433	15.95	5	12	50	5	55	79	1260	1260	363.80	0.003	0.22	CU				1.77
MCD0435	81.29	5	446	3891	5	3896	76	6178	2247	462.54	0.005	0.16	P*	5 to 92	0.99	0.75	1.69
MCD0437	15.81	5	50	686	5	691	207	3272	3272	249.80	0.013	0.83	P*	5 to 50	0.99	1.84	3.80
MCD0446	28.18	5	48	413	5	418	90	2536	2536	490.70	0.005	0.18	CU				1.83
MCD0478	22.39	5	43	405	5	410	103	2306	2306	465.60	0.005	0.22	CU				2.23
MCD0484	56.64	8	234	1726	5	1731	58	3285	1554	523.00	0.003	0.11	P		0.99	0.89	2.11
MCD0488	101.42	5	474	3886	5	3891	76	7708	6258	441.30	0.014	0.17	P		0.99	0.79	1.59
MCD0491	17.55	5	56	660	5	665	291	5108	5108	327.60	0.016	0.89	P		0.96	1.23	2.25
MCD0496	29.96	5	92	958	5	963	144	4314	3351	367.80	0.009	0.39	P*	5 to 137	0.99	1.02	2.94
MCD0533	29.53	5	73	633	5	638	160	4725	4087	352.04	0.012	0.45	P		1.00	1.10	1.82
MCD0539	46.67	5	240	1945	5	1950	66	3080	1130	232.35	0.005	0.28	P*	5 to 40	0.98	1.62	1.64
MCD0545	37.00	11	52	178	6	184	17	629	629	411.00	0.002	0.04	P*	5 to 107	0.99	0.73	1.21
MCD0562	20.48	5	30	155	5	160	33	676	676	381.00	0.002	0.09	P*	5 to 48	0.98	1.11	1.48
MCD0591	48.35	5	255	2682	5	2687	139	6720	2658	348.30	0.008	0.40	P*	5 to 87	0.99	1.30	1.51
MCD0625	24.28	5	55	426	5	431	69	1675	1244	400.00	0.003	0.17	P		0.98	1.27	2.26

HoleID, drill core number; mean, mean of vein thickness (mm); mode, mode of vein thickness (mm); SD, standard deviation of vein thickness; range, range of vein thickness (mm); min, minimum vein thickness measured (mm); max, maximum vein thickness measured (mm); *N*, number of veins measured; L_f, length of drill core sampled (m); sum (all), sum of the true thickness of measured fault-fill and subsidiary veins (mm); sum (sub), sum of the true thickness of measured subsidiary veins (mm); *e* (sub), vertical extensional strain for subsidiary veins; *d* (vein/m): vein density; CFT, cumulative frequency of vein thickness; P, power-law; P*, power-law with departure; CU, convex upwards; lin. int., linear interval of CFT; *r*, regression coefficient; D_t, exponent of the CFT; C_v, coefficient of variation of vein spacing of the fault-fill and subsidiary veins.

represent infill of open space due to vertical extension during deformation, the aggregated vein thickness measured parallel to vein opening directions (assumed sub-vertical) provides an estimate of the bulk vertical extensional strain (e) of the deformation event. Bulk vertical extensional strain (e) is given by:

$$e = \left(L_f - L_i\right)/L_i \quad (1)$$

where L_f is the thickness of subsidiary veins plus pre-failure rock (the length of the measured drill core) and L_i is the thickness of rock prior to failure and emplacement of subsidiary veins (cf. Foxford et al., 2000). The fault-fill veins in west dipping reverse faults represent infill of dilatational sites along the fault surface and also the juxtaposition of vein segments during progressive fault zone development. Since fault-fill veins are not necessarily emplaced as a result of *in situ* dilation in a vertical direction they have been filtered from the calculation of e. In drill cores, the fault-fill veins were determined from their moderately dipping orientation, laminated and styolitic internal texture and spatial distribution with respect to the inferred positions of the Lords, Walters and Thompson faults. Derived e have been contoured and anomalously high e values that are greater than 0.005 define a northwest trending area of about 300 m width between the Walters and Thompson faults corresponding with the Walters fault tip (Fig. 9a).

Staircase plots portray the cumulative vein thickness plotted against distance along a drill core and are a simple measure of the distribution of bulk extensional strain (Gillespie et al., 1999). Over the same length of core a steeper gradient in cumulative vein thickness indicates relatively greater extensional strain. The smoothness of the cumulative vein thickness curve reflects whether the strain is distributed on a high number of relatively small thickness veins (smooth curve) or on a smaller number of relatively thick veins (stepped curve). Staircase plots have been derived for drill cores that define sections that are parallel and perpendicular to the zone of high e (Figs. 9a and 10). In the section perpendicular to the zone of high e, two drill cores spaced about 100 m apart have relatively steep but smooth gradients and define a zone of high vertical extensional strain at the Walters fault tip (Fig. 10). Gradients of staircase plots outside of this zone are flat with steps that correspond to the Walters vein (Fig. 10).

On a section parallel to the zone of high e, relatively steep but smooth gradients occur on plots of two cores at the Walters fault tip and indicate that relatively high, evenly distributed extensional strain occurs about 300 m into the hanging wall of the Lords fault (Fig. 10b). Plan contoured values of e (Fig. 9a) indicate that extensional strain remains high further into the hanging wall of the Lords and Walters faults but a staircase plot indicates that the extensional strain is heterogeneously distributed in the vicinity of the Thompson fault (Fig. 10b). The Thompson fault-fill vein occurs at this locale and has associated subsidiary veins of anomalous thickness. Evenly distributed extensional strain is relatively high in the immediate footwall of the Lords fault decreasing to relatively low levels about 150 m into the footwall (Fig. 10b).

6.3. Vein density

Vein density is defined as the number of subsidiary veins per interval of drill core. Summary vein densities were calculated using the total length of individual drill cores and the results contoured in plan view (Fig. 9b). The values obtained vary between 0.04 and 0.89 and have a skewed distribution (Fig. 9b inset). Anomalously high values of vein density that are greater than 0.20 define a northwest trending area of about 200 m width between the Lords and Thompson faults corresponding with the Walters fault tip (Fig. 8b).

Vein density in section was examined by dividing each drill core into 10 m intervals and calculating the subsidiary vein density for each interval. Three sections that were parallel to the zone of anomalous high vein density in plan are derived from the data (Fig. 11a). These sections were chosen to illustrate vein distribution relationships within and external to the anomalous zone. Intervals of high vein density that exceed values of 1.5 occur mostly within the anomalous zone at the Walters fault tip (Fig. 11c). Intervals of moderate vein density with values between 0.5 and 1.5 mostly occur within the anomalous zone but are also found around faults and as isolated zones in the hanging wall of the Lords fault (Fig. 11b–d). Intervals of low vein density that have values less than 0.5 are observed throughout the analysed drill cores (Fig. 11b–d). Within the anomalous zone the density of subsidiary veins is higher at the Walters fault tip than at the Thompson fault (Fig. 11c).

6.4. Statistics and spatial properties of veins

Over 1900 measurements of gold-associated veins were made in the analysed drill cores at Centenary. The thicknesses of gold-associated veins within the drill cores range from the measured minimum thickness of 5 mm to 3.90 m (Table 2). The thickest measured veins correspond to the fault-fill veins. Stickplots of Gillespie et al. (1999) are used to spatially illustrate the properties and distribution of gold-associated veins (Fig. 12). Stickplots show a bar at the intersection of a vein with the length of the bar representing the veins thickness. In this study, the width of the bar indicates the interval of drill core that the vein occupies. Stickplots were derived for drill cores that define sections perpendicular and parallel to the zone of high e and vein density (Fig. 9a). The subsidiary veins outside of the zone of high e and vein density have a smaller range in thickness than those within the zone (Fig. 12a). Within the zone there are less anomalously thick subsidiary veins at the Walters fault tip compared to near the Thompson fault (Fig. 12b). Stickplots on the section show that gold-associated veins occur in the Mount Pickering dolerite and overlying volcanosedimentary rocks (Fig. 12).

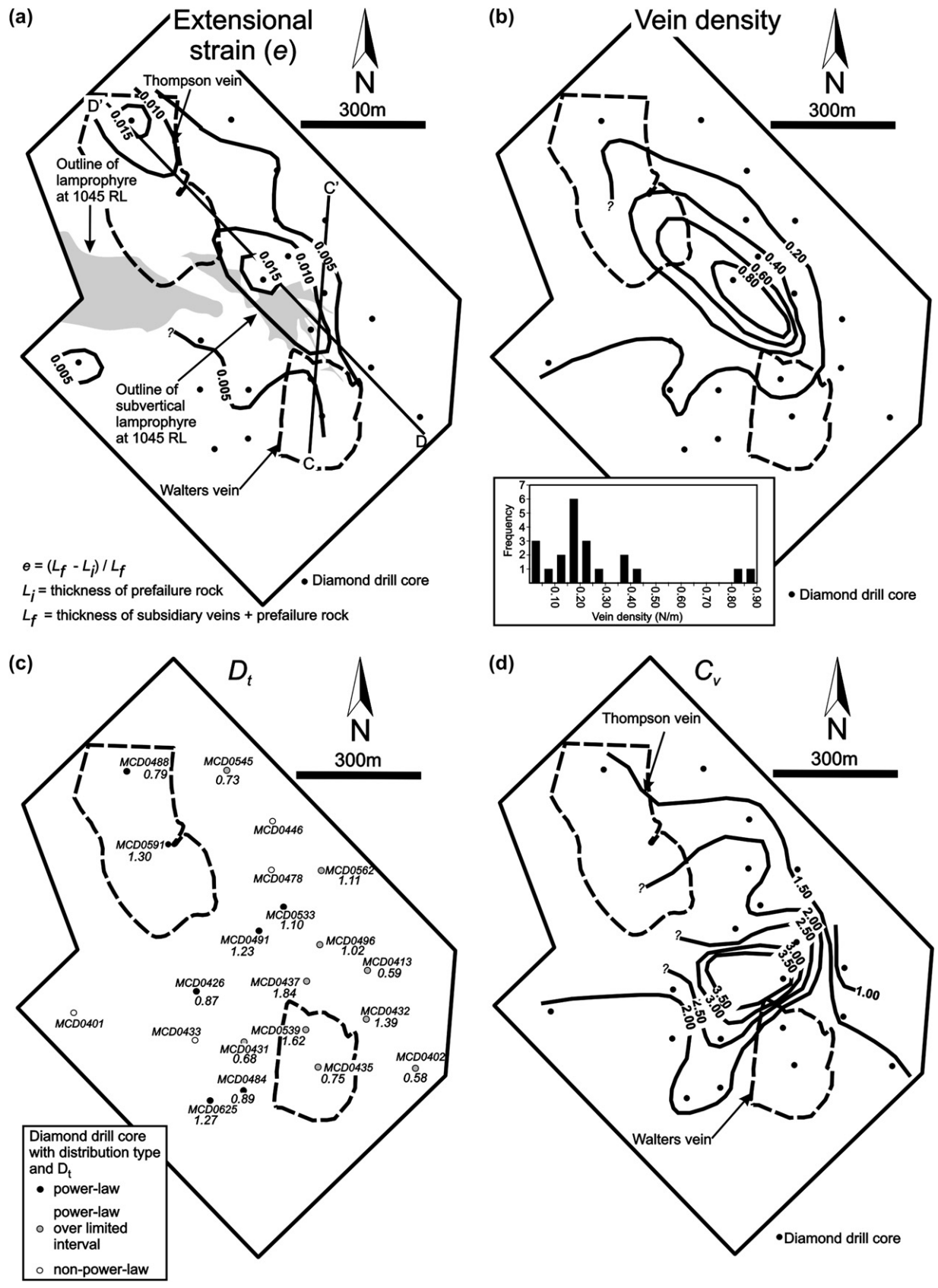

Fig. 9. Contoured distributions of: (a) Bulk vertical extensional strain (e) for subsidiary veins. An area of anomalous e greater than 0.005 occurs between the Walters and Thompson veins. Projection of sub-vertical lamprophyres at the 1045 RL are also shown. (b) Vein density which shows a similar anomaly to that defined by e. Inset shows frequency of vein density for examined drill cores at Centenary. (c) Exponent of cumulative frequency of vein thickness (D_t) with contours of e also shown. (d) Coefficient of variation of vein spacing (C_v). All strain and vein distribution indicators show highest values at the Walters fault tip. Also shown are outlines of the Walters and Thompson fault-fill veins and locations of drill cores used in this study. Thick borders on the diagrams correspond with area marked on Fig. 2.

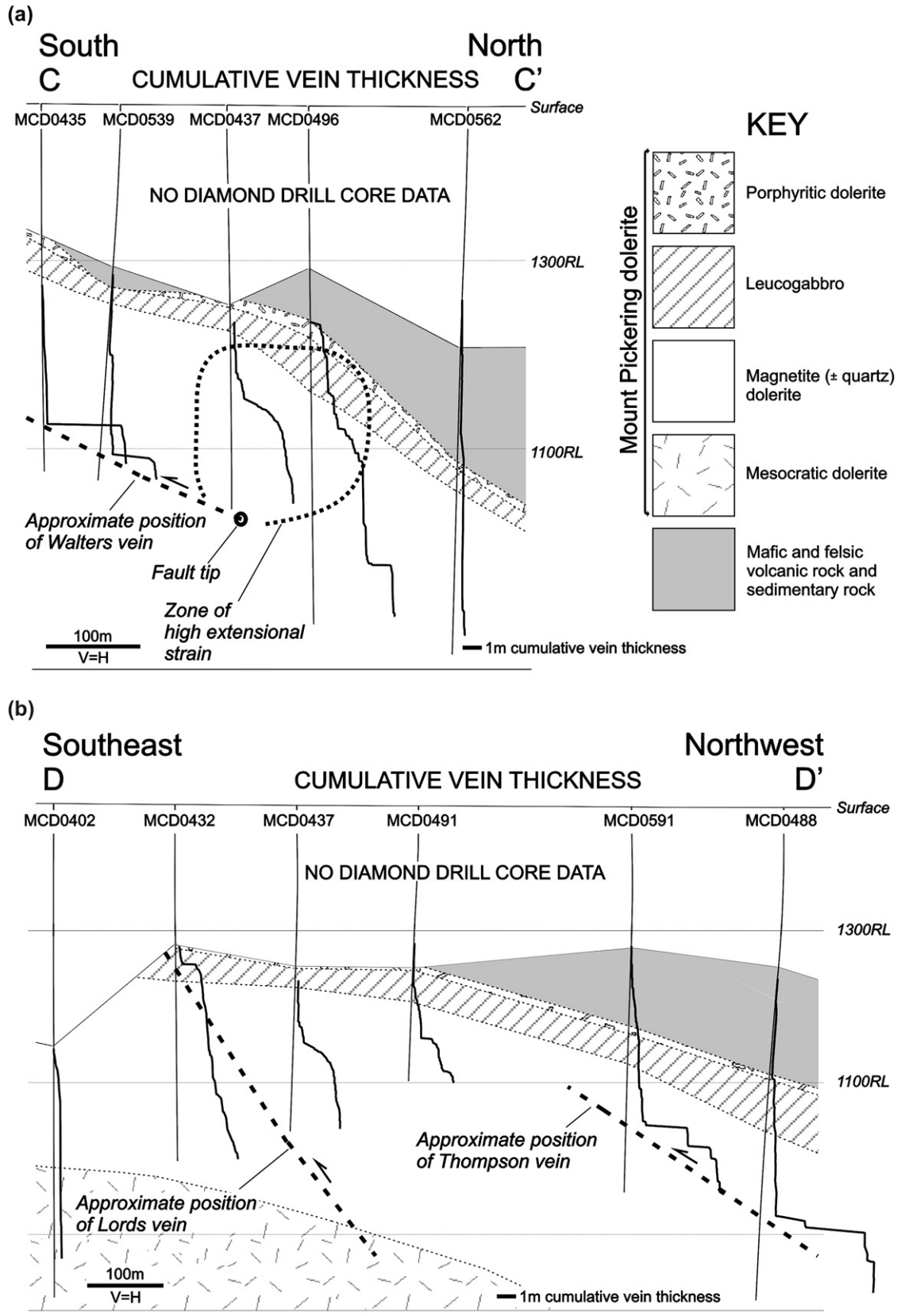

Fig. 10. Plots of cumulative vein thickness for drill cores along sections through the zone of high bulk vertical extensional strain (e) at the Centenary orebody. For location of sections see Fig. 9. (a) North-south section parallel to the Walters fault. (b) Northwest-southeast section sub-parallel to the zone of high e.

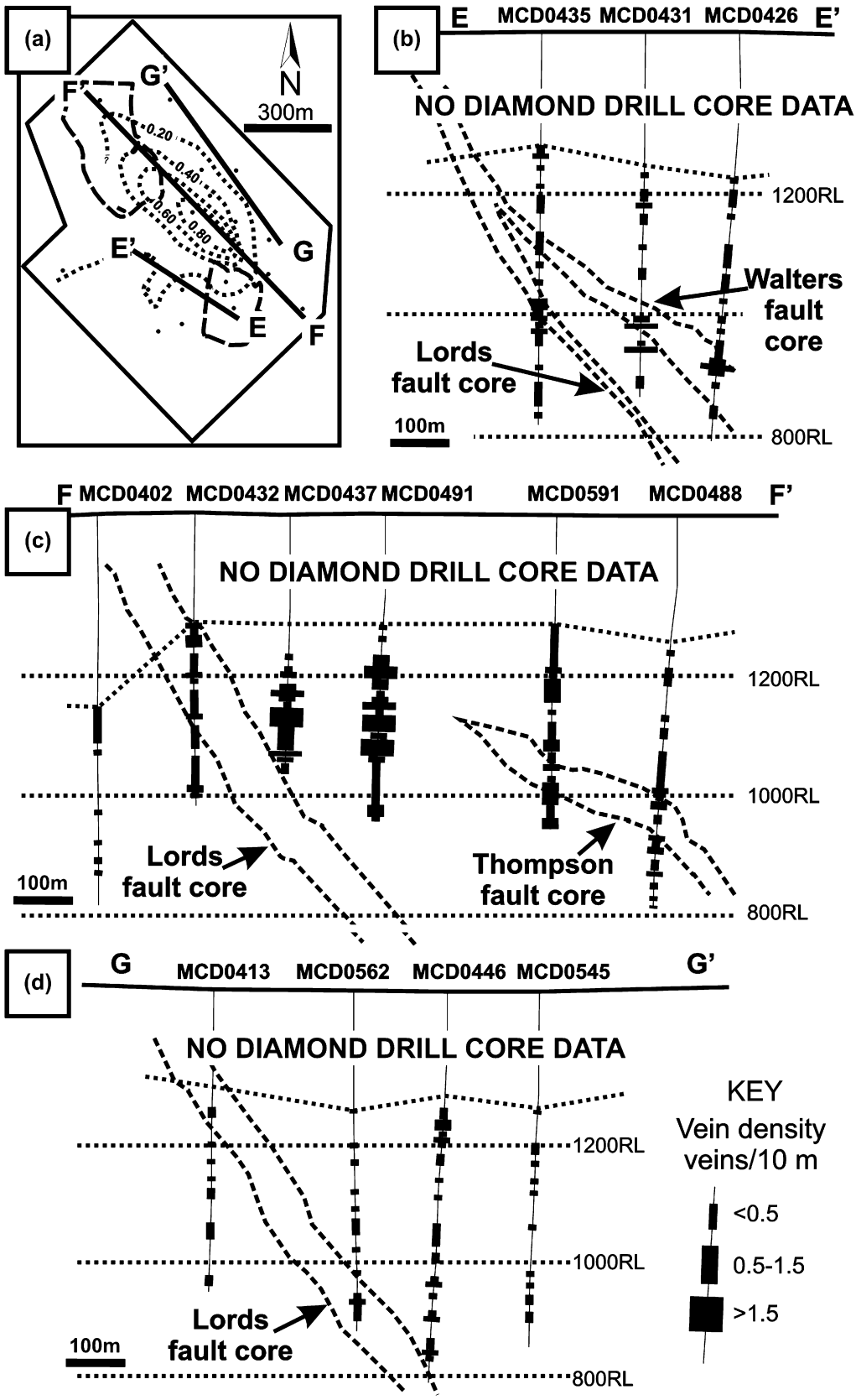

Fig. 11. Sections showing distribution of vein density at the Centenary orebody. (a) Plan showing locations of sections, contoured vein density and outlines of the Walters and Thompson fault-fill veins. (b) Section showing distribution of vein density to the southwest of the zone of high vein density. (c) Section showing distribution of vein density in the zone of high vein density. (d) Section showing distribution of vein density to the northwest of the zone of high vein density.

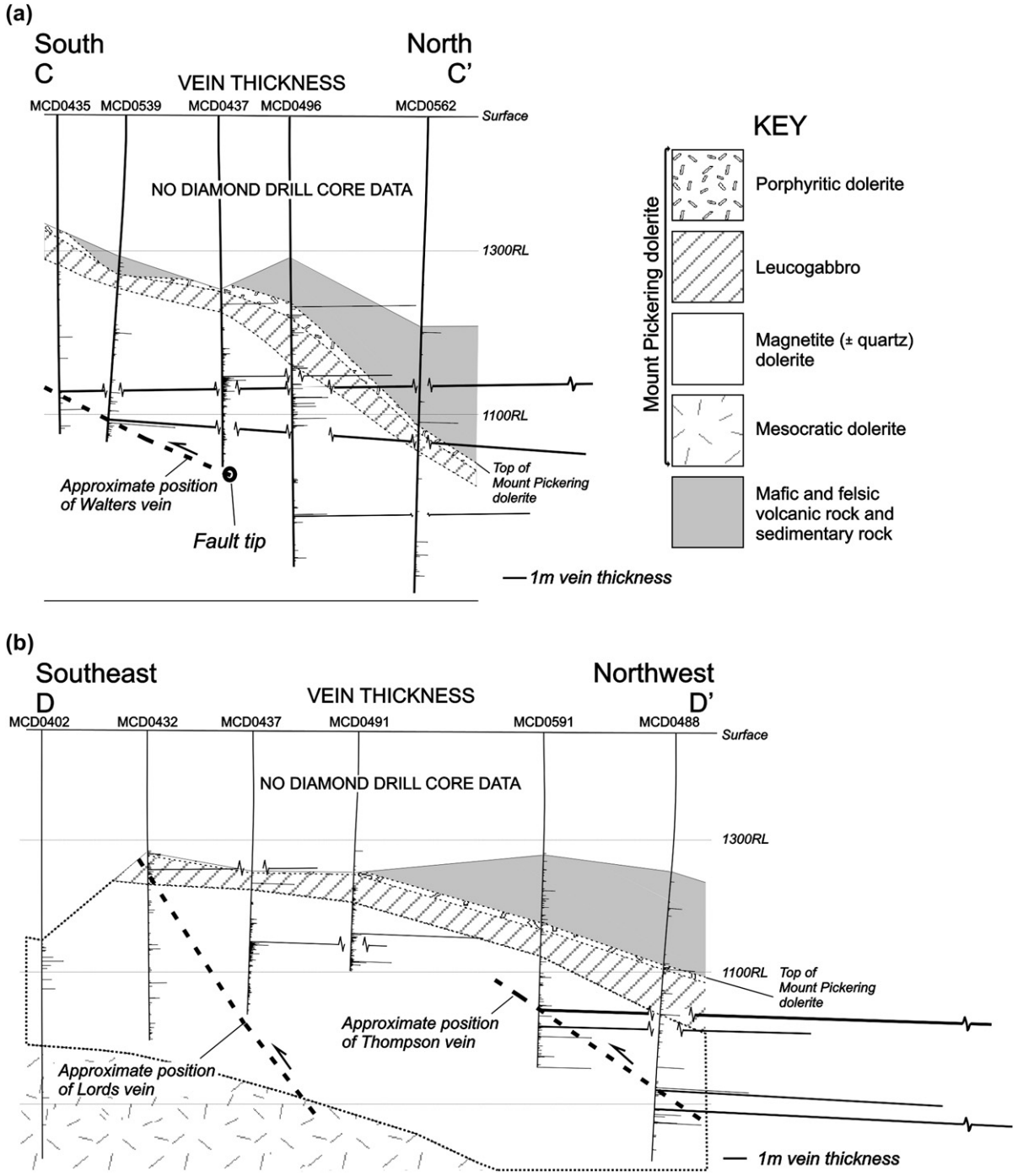

Fig. 12. Sections across the zone of high bulk vertical extensional strain (e) showing the distribution of veins and vein thickness at the Centenary orebody. The length of a bar represents vein thickness and the location of the interval over which the vein was recorded. For location of sections see Fig. 9. (a) North-south trending section parallel to the Walters fault and across the zone of high bulk vertical extensional strain (e). See text for discussion. (b) Northwest-southeast trending section sub-parallel to the zone of high e at the Walters fault tip. See text for discussion.

6.5. Cumulative vein thickness and vein width distribution

Plots of true vein thickness against cumulative frequency on log-log plots have straight lines when they conform to a power-law relationship:

$$N_t \propto t^{-Dt} \tag{2}$$

where N_t, termed the cumulative number, is the number of veins equal to or greater than thickness t, t is the vein thickness and $-D_t$, referred to as the exponent of the cumulative frequency of vein thickness, is the slope of the log-log plot (Sanderson and Roberts, 1994; Gillespie et al., 1999). Higher values of D_t indicate a greater proportion of thinner veins. Vein thickness systematics for the individual drill cores analysed at Centenary are varied, with power-law distributions and

distributions of convex upward form (Figs. 13–15). In general, higher values of D_t are observed for drill cores at the Walters fault tip (Fig. 9c), indicating a greater proportion of relatively thinner subsidiary veins at this locale. This reflects that the deformation is more distributed at the fault tip. The measured D_t at Centenary (0.58–1.84) are comparable to exponents reported for other mineralised vein arrays (0.49–1.24; Gillespie et al., 1999) with some exceptionally high values (>1.2) at the Walters fault tip.

6.6. Coefficient of variation of vein spacing and clustering of veins

The coefficient of variation of vein spacing, C_v, is a measure of the clustering of veins along a line and is defined as:

$$C_v = \mathrm{SD}(s)/s \quad (3)$$

where SD(s) is the standard deviation of vein spacing and s is the mean vein spacing (Gillespie et al., 1999). Random spacings of veins have $C_v = 1$; $C_v > 1$ indicates veins are clustered and $C_v < 1$ indicates that veins are anti-clustered or regularly spaced (Gillespie et al., 1999). Coefficients of variation of vein spacing for the 21 drill cores calculated including fault-fill and subsidiary veins, range from 0.87 to 3.80. However, only one drill core has $C_v < 1$. Higher values of C_v occur in drill cores at the Walters fault tip (Fig. 9d).

7. Distribution of veins in rock types at Centenary

In general, it is observed that veins at Centenary are best developed in felsic volcanic rock, are well developed in the Mount Pickering dolerite, volcanosedimentary rocks and granitoids and are poorly developed in lamprophyric rocks (Krcmarov et al., 2000). This has two implications. First is that the volume of rock with high e and vein density is slightly over-estimated because the irregular lamprophyric body occurs within this zone but is unaccounted for due to the spacing of analysed drill cores being greater than the thickness of the body (Fig. 9b). The second implication is that the Walters fault-fill vein splays into an array of subsidiary veins within magnetite (± quartz) dolerite. In detail, it is an intrusive breccia within the magnetite (± quartz) dolerite that spatially correlates most closely with the fault tip. This breccia comprises enclaves of felsic volcanic rock and irregular bodies of lamprophyre. As veins are generally well developed in felsic volcanic rock the intrusive breccia may, therefore, have been important for the localisation of subsidiary veins at Centenary.

8. Synthesis of the relationships of faults and subsidiary veins

All analysed drill cores at Centenary contain subsidiary veins, although subsidiary vein abundances are relatively

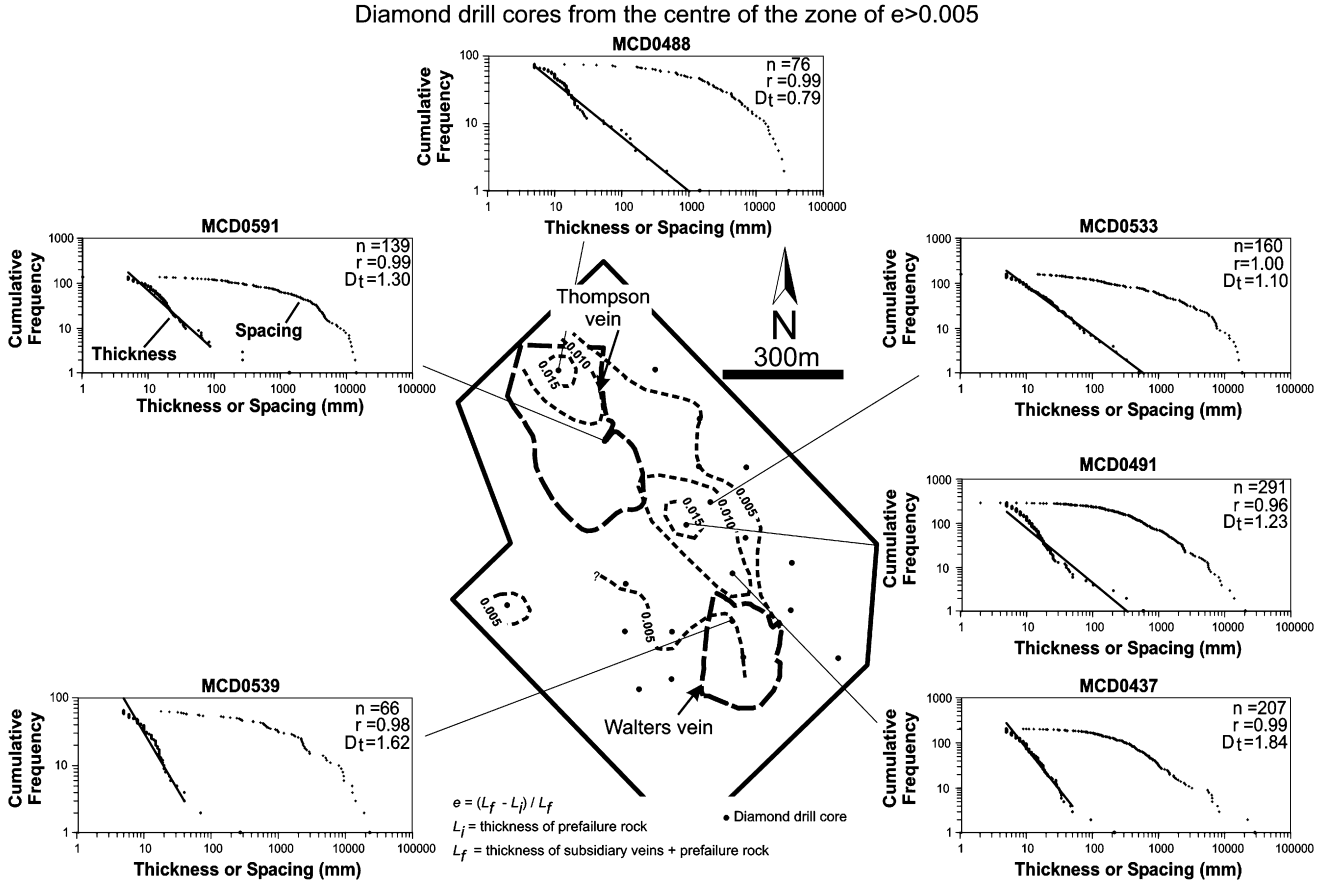

Fig. 13. Cumulative frequency versus thickness and spacing plots for vein distributions from the centre of the zone of $e > 0.005$.

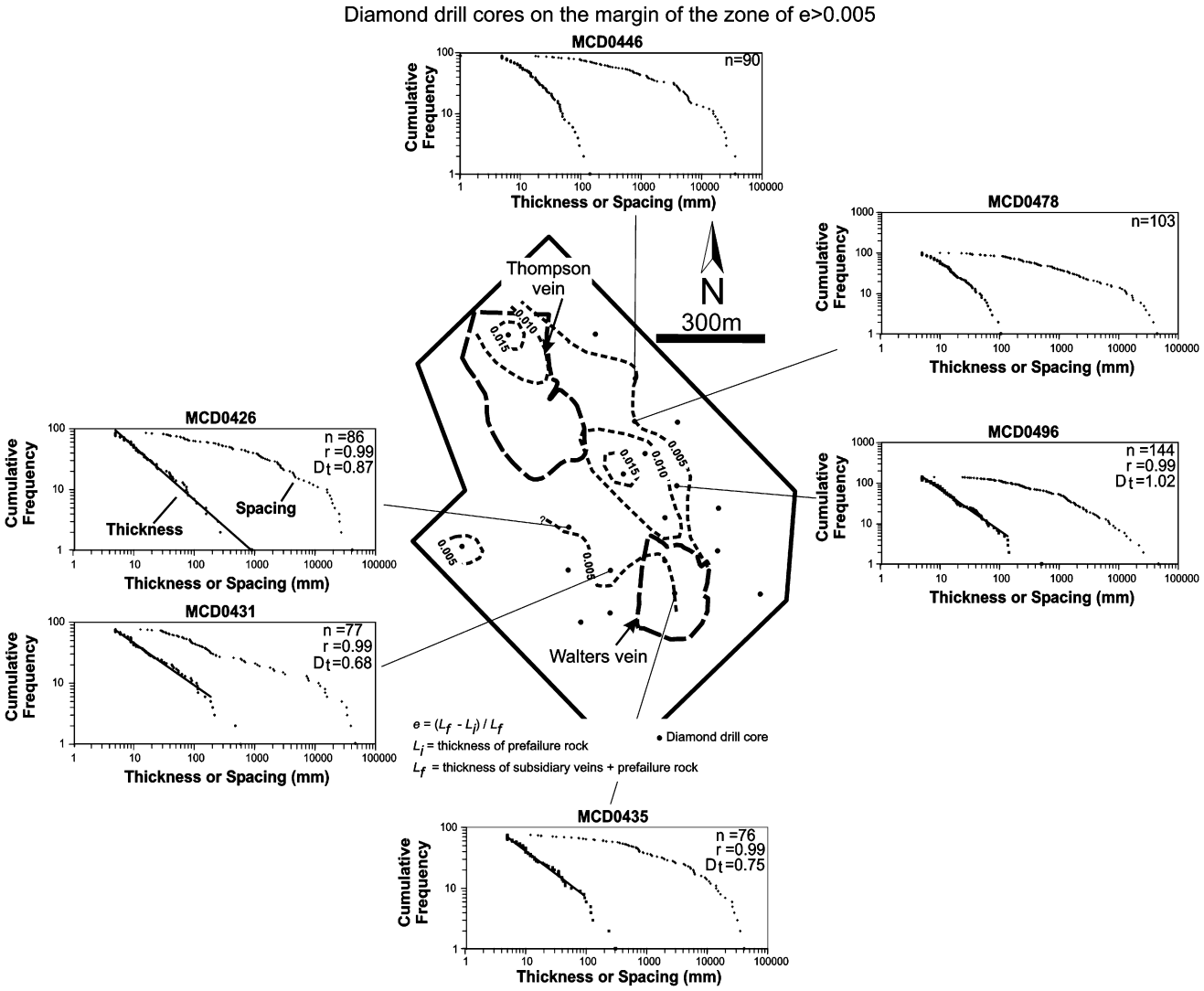

Fig. 14. Cumulative frequency versus thickness and spacing plots for vein distributions on the margin of the zone of $e > 0.005$.

low away from recognised faults. Therefore, a background level of fracture or strain exists at Centenary although the relationship to faults cannot be fully evaluated at the scale of the present study. There is, however, a clearly defined 200–300 m wide tabular zone of anomalously high e and vein density relative to surrounding rock. This zone links the Lords–Walters and Thompson faults and represents a zone of damage between these faults. The highest recorded e and vein density suggest that damage is localised at the Walters fault tip (Fig. 16). At the fault tip, the vertical thickness of the zone is about 150–250 m but the zone becomes less well constrained near the Thompson fault. Stickplots (Fig. 12b) and sections of vein density (Fig. 11c) indicate that damage about the faults is asymmetric, with an anomalous number and volume of subsidiary veins in the hanging wall of the Lords fault (Fig. 16).

Within the damage zone, vertical extensional strain at the Walters fault tip is distributed on a high number of relatively small, clustered subsidiary veins as indicated by stickplots (Fig. 12), higher values of D_t (Fig. 9c) and C_v values greater than one (Fig. 9d). Near the Thompson fault there are more subsidiary veins of anomalous thickness and the density of veins is lower. Isolated intervals of low vein density extend into the hanging wall of the Thompson fault. Coefficients of variation at small vein thickness thresholds at Centenary are greater than one and particularly high at the fault tip. Coefficients of variation greater than one imply vein clustering and suggest that the formation of a new vein was more probable near an existing vein (Gillespie et al., 1999). Underground exposures within the damage zone support vein interaction with veins of complex geometries forming networks within the damage zone (Fig. 8). Many subsidiary veins occur as wing crack arrays at the tips of faults (cf. Fig. 5), indicating a structural and hydraulic link between the veins.

The systematic spatial relationships between the distribution and properties of gold-associated, subsidiary veins and reverse faults suggests a causal relationship between the localisation and formation of the subsidiary veins and the faults. The localisation and decrease in subsidiary structures with distance from the Walters fault tip is consistent with failure

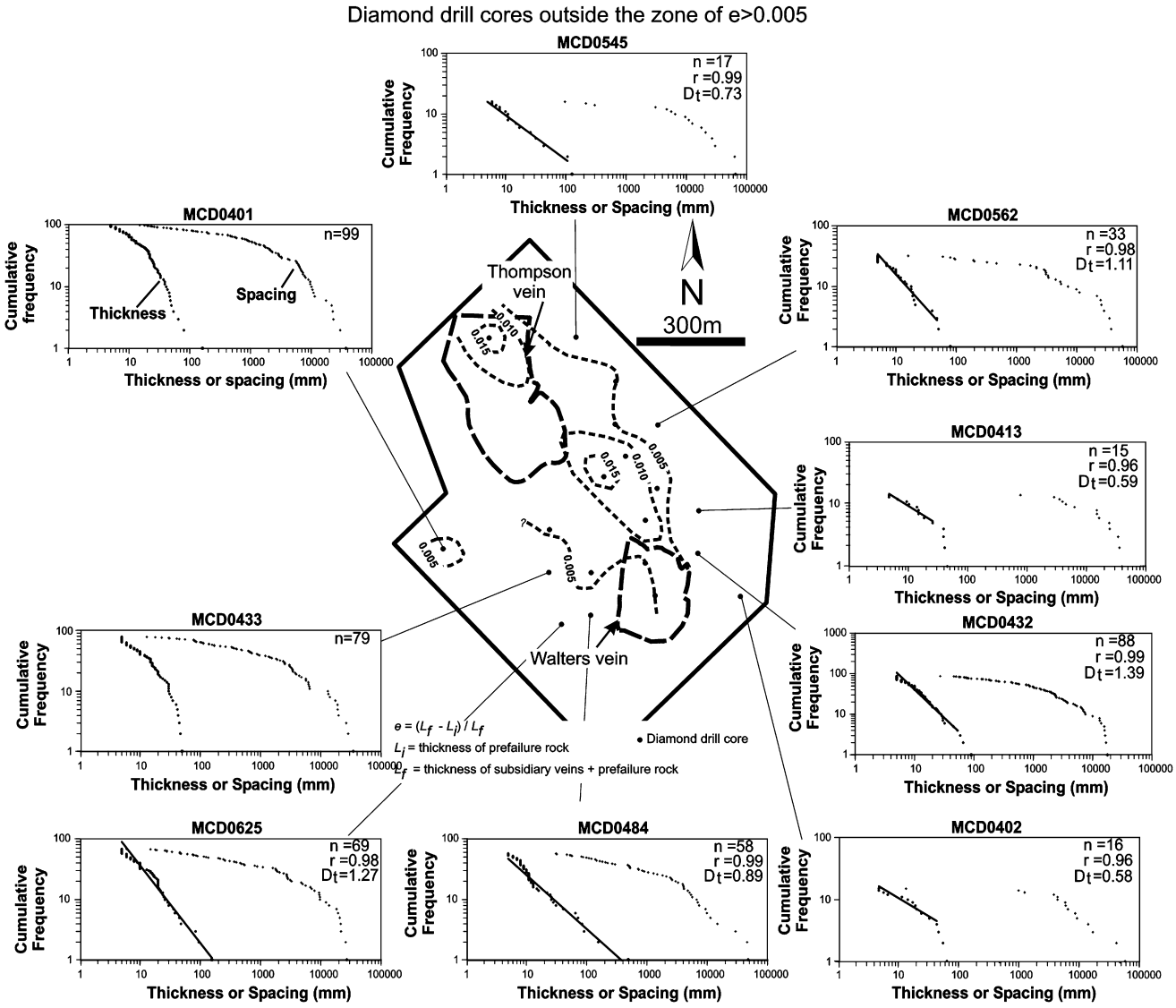

Fig. 15. Cumulative frequency versus thickness and spacing plots for vein distributions outside the zone of $e > 0.005$.

due to anomalous stress states and volume problems predicted by numerical models at fault tips (Segall and Pollard, 1980; Harris and Day, 1993; Zhang and Sanderson, 1996). Wing crack arrays of subsidiary veins within this zone (Fig. 5) highlight the requirement for structural compatibility within this zone to accommodate the overall slip on the major reverse faults (cf. Rispoli, 1981). The highest values of e occur at the Walters fault tip and indicate that the greatest dilation occurred there. At the orebody scale, no clear spatial relationship exists that suggests subsidiary veins are localised by steeply dipping faults, despite some subsidiary veins fringing steeply dipping faults in underground exposures. The relationship of steeply dipping faults to west dipping reverse faults and in particular the Walters fault tip is ambiguous. The recognised high abundance of steeply dipping faults in the damage zone may be an artefact of the high amount of data obtainable from underground exposures in this area and not necessarily indicate a dominant control of the dynamics of the evolution of one geometrical fault set on another.

9. Gold distribution in the Centenary fault system

In subsidiary veins, gold occurs in native form and with pyrite ± pyrrhotite ± chalcopyrite ± magnetite. Gold also occurs in wall rock around the veins that has been hydrothermally altered to ankerite-white mica ± pyrite ± pyrrhotite. Within the hydrothermally altered wall rock gold occurs as isolated grains in the ankerite-white mica ± pyrite assemblage, along the margins of pyrite and as inclusions within pyrite and pyrrhotite.

The linking damage zone with anomalous number and volume of subsidiary veins correlates closely with the Centenary gold resource (Fig. 17). An important control on the distribution of subsidiary veins appears to be the magnetite (± quartz) dolerite in the Mount Pickering dolerite and particularly an intrusive breccia within this unit. A similar lithological control is also observed for Mount Charlotte-style gold mineralization that is associated with veins in the Unit 8, quartz-rich dolerite at Kalgoorlie, Western Australia (Travis et al., 1971). This

may reflect the competence of these quartz-rich dolerite units relative to other zones within the differentiated dolerites and other greenstone belt rocks.

A comparison was made between vein density and gold grade at Centenary. Vein density was calculated over 10 m intervals of drill core. The same 10 m interval of drill core, including veins and unaltered and altered wall rocks, was analysed for gold at metre spacing and compiled into a 10 m composite. The plot between gold grade and vein density shows considerable scatter of the data (Fig. 17). Anomalous gold grades do not always correlate with the locations of individual veins, areas containing numerous veins or veins of significant thickness. This is indicated by comparison of sections showing stickplots and gold grade (Fig. 17). At the orebody scale the distribution of gold matches the distribution of subsidiary veins, however, in detail a simple one to one correlation is not observed between gold grade and the number or thickness of subsidiary veins. In part, this may be explained by the patchy distribution of gold hosted within veins and in wall rock hydrothermal alteration zonations, which results in considerable variation in analysed gold grade even within a single sample. For example, the range for a powdered sample of a subsidiary vein and surrounding wall rock hydrothermal alteration analysed by graphite furnace atomic absorption spectrometry three times was 18 ppm.

In summary, at the 200–300 m scale of the Centenary orebody gold grade is spatially related to the linking damage zone but individual veins and vein arrays on the tens of metre scale do not always correlate with high gold grade.

10. Fluid flow in the Centenary fault system

High flux, fracture-related fluid flow is favoured when and where fracture apertures, density and connectivity are highest (Cox et al., 2001). Estimates of gold and quartz solubility under hydrothermal conditions suggest that formation of an economically important gold-quartz vein system requires the passage of large fluid volumes (cf. Sibson, 2004). High vein density and vertical extensional strain and the clustering and connectivity of subsidiary veins in the damage zone at the Walters fault tip suggests this was a zone of high fracture-related permeability and porosity (Fig. 16). The spatial correlation of the Centenary gold orebody with the damage zone is consistent with this region having had the passage of large volumes of gold-bearing hydrothermal fluid. At a first approximation, therefore, the location of the Centenary orebody is predictable.

The brittle nature of structures failing during gold mineralisation at Centenary and the laminated internal structure of fault-fill veins on reverse faults suggests that deformation during gold mineralisation occurred within the seismogenic regime and strain was accrued through episodic failure events (Sibson et al., 1988; Cox, 1995; Robert et al., 1995). The hydrological importance of seismogenic fault zone components varies with the evolution of a fault zone through time (Chester et al., 1993). The temporal permeability of damage zone fracture networks and the fault core can be intimately related but vary significantly from each other throughout a seismic cycle (Sibson et al., 1988; Chester et al., 1993; Cox, 1995; Robert et al., 1995; Sibson and Scott, 1998). Fault cores can have low permeability and be effectively sealed to fluid flow prior to rupture events, due to the presence of impermeable fault rocks and hydrothermal mineral precipitates, but become high permeability fluid conduits following fault rupture when the sealing fault rocks and hydrothermal minerals are disaggregated by slip along the fault (Sibson et al., 1988; Cox, 1995; Robert et al., 1995). Prior to fault rupture, fluid impeded by structural traps and sealed fault cores may reach supralithostatic pressures and cause hydraulic fracturing and development of adjacent extensional fracture networks (Cox, 1995; Robert et al., 1995). Also, the opening of subsidiary structures about the fault core is favoured by the increase in pre-seismic strain along the fault zone preceding fault rupture (Bruhn et al., 1990). Expulsion of fluids and closing of subsidiary structures is likely to accompany fault rupture when fluids are redistributed along high permeability fault cores that provide access to lower pressure fluid compartments (Sibson et al., 1988; Cox, 1995; Robert et al., 1995). The spatial variability of subsidiary veins about the Lords, Walters and Thompson faults suggests that these were important conduits controlling the temporal supply and release of fluids from the linking damage zone. However, as discussed below the temporal permeability of the faults and linking damage zone at Centenary may differ from the case where the damage zone of strain flanks the fault core.

Aftershock clustering and post-failure strain accommodation at dilatational linkage zones in active fault systems follow fault rupture (Sibson, 1985; Peltzer et al., 1996) indicating that subsidiary failure events follow major fault ruptures in some fault zone settings. By analogy the subsidiary failure events in the damage zone at the Walters fault tip may have followed major rupture events and high-flux fluid flow on the west dipping reverse faults. Fluid transmission within the damage zone would, therefore, follow high flux flow on fault cores making the damage zone a temporary high fracture-related porosity and permeability zone within a volume of otherwise low porosity-permeability rock. The presence of wing crack arrays supports the interpretation of high fluid pressures within the linking damage zone (cf. Barquins and Petit, 1992). Fluids within domains of sub-horizontal fracture networks bounded by vertically extensive fault cores that are sealed will not be able to move to lower pressure compartments at higher crustal levels. Trapped fluids may drive fluid-induced failure of the rock mass, accounting for clustering of veins, or diffuse into, and react with, rock at the fracture walls producing well-defined hydrothermal alterations, such as are seen at the Centenary orebody (cf. Gardner et al., 2001). The time-span of fluid transmission within the damage zone would relate to strain accommodation on the adjacent fault segments but is likely to occur over longer time intervals than failure on the major fault segments (Peltzer et al., 1996). Longer time intervals for fluid transmission favour fluid permeation into wall rock and time-dependent alteration reactions that may cause gold deposition. The time-integrated effect of the

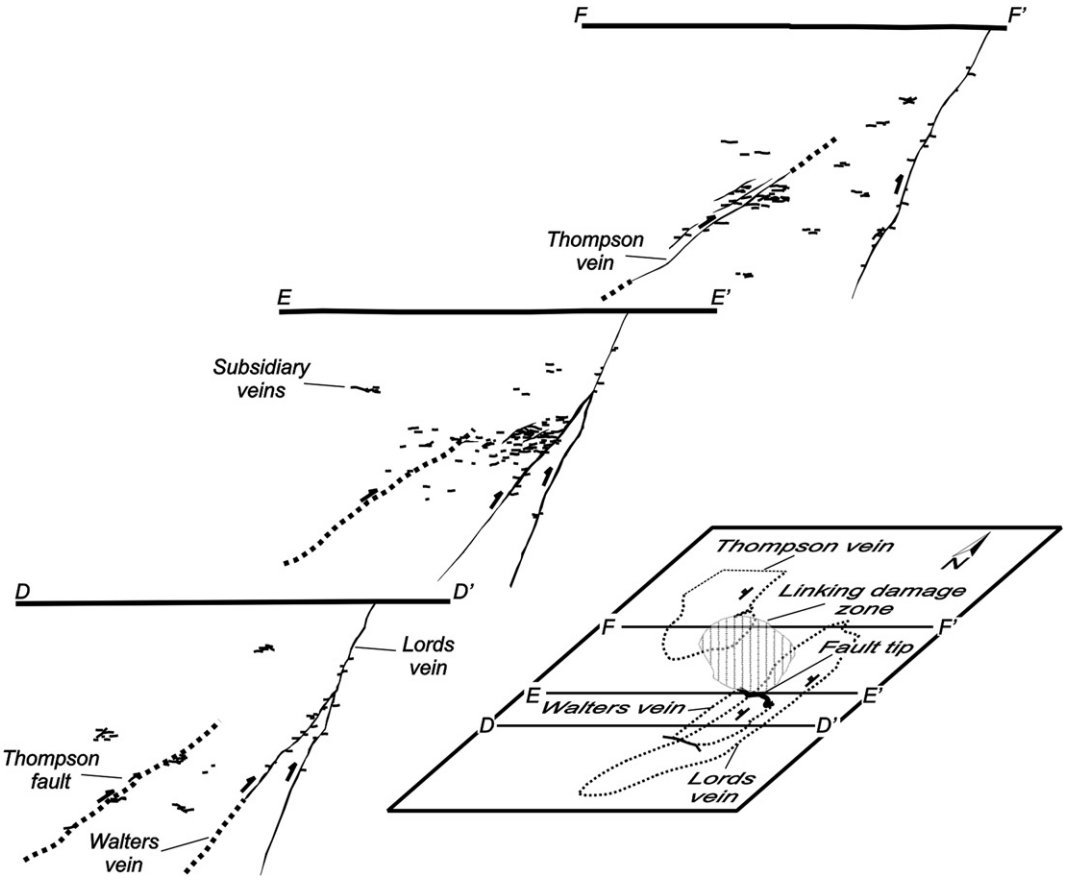

Fig. 16. Schematic sections showing the distribution of reverse faults and subsidiary veins at the Centenary orebody.

baffling of fluxing gold-bearing fluids within lower-order subsidiary structures at Centenary may have resulted in a much higher efficiency of gold removal from hydrothermal fluids and hence contributed to formation of the Centenary gold orebody.

11. Conclusions

Moderately (~45°) west dipping, reverse and steeply dipping predominately northeast to east and, to a lesser extent, east to southeast striking faults failed during gold mineralisation at Centenary in response to sub-horizontal east-west shortening and sub-vertical extension. Both sets of faults have lengths of several hundred metres to kilometres. Damage zones comprising gentle dipping veins, are temporally, genetically and locally spatially related subsidiary structures to west dipping reverse and steeply dipping faults.

Analysis of subsidiary vein distributions at Centenary indicates background levels of subsidiary veins at the orebody that are not clearly related to faults at the scale of the present study. However, a 200–300 m wide tabular damage zone links major west dipping faults and is localised at the tip of one such fault. This damage zone is clearly defined by anomalies of bulk vertical extensional strain and vein density. Damage around the west dipping faults is asymmetric being largely confined to the hanging-wall of the Lords fault. Within the damage zone high vein densities, large power-law exponents and limited variations in subsidiary vein thickness suggest that vertical extensional strain at the fault tip is distributed on a high number of relatively small thickness, clustered veins. Vein density and power-law exponents decrease with distance from the fault tip and an increasing number of anomalously thick subsidiary veins are observed. However, overall bulk vertical extensional strain remains high indicating that subsidiary vein material is concentrated on a higher number of anomalously thick veins.

Strain localisation within the damage zone is complex with coefficients of variation greater than one implying clustering of gold-associated veins. Curviplanar, intersecting networks of subsidiary veins in underground exposures suggest fracture interaction was important in the formation of the veins. The systematic variations in the distribution and properties of subsidiary veins around west dipping faults and in particular the fault tip suggest that these faults imparted a strong control on vein localisation. At the deposit scale the distribution of subsidiary veins is not related to steeply dipping faults although locally subsidiary veins fringe the faults. At the orebody scale the distribution of gold matches the distribution of subsidiary veins although within the damage zone a simple relationship is not observed between gold grade and the number or thickness of subsidiary veins. The complex relationship between gold grade and the number or thickness of subsidiary veins is not completely resolved but may in part be due to difficulties in sampling the gold that is erratically distributed in veins and surrounding hydrothermal alteration.

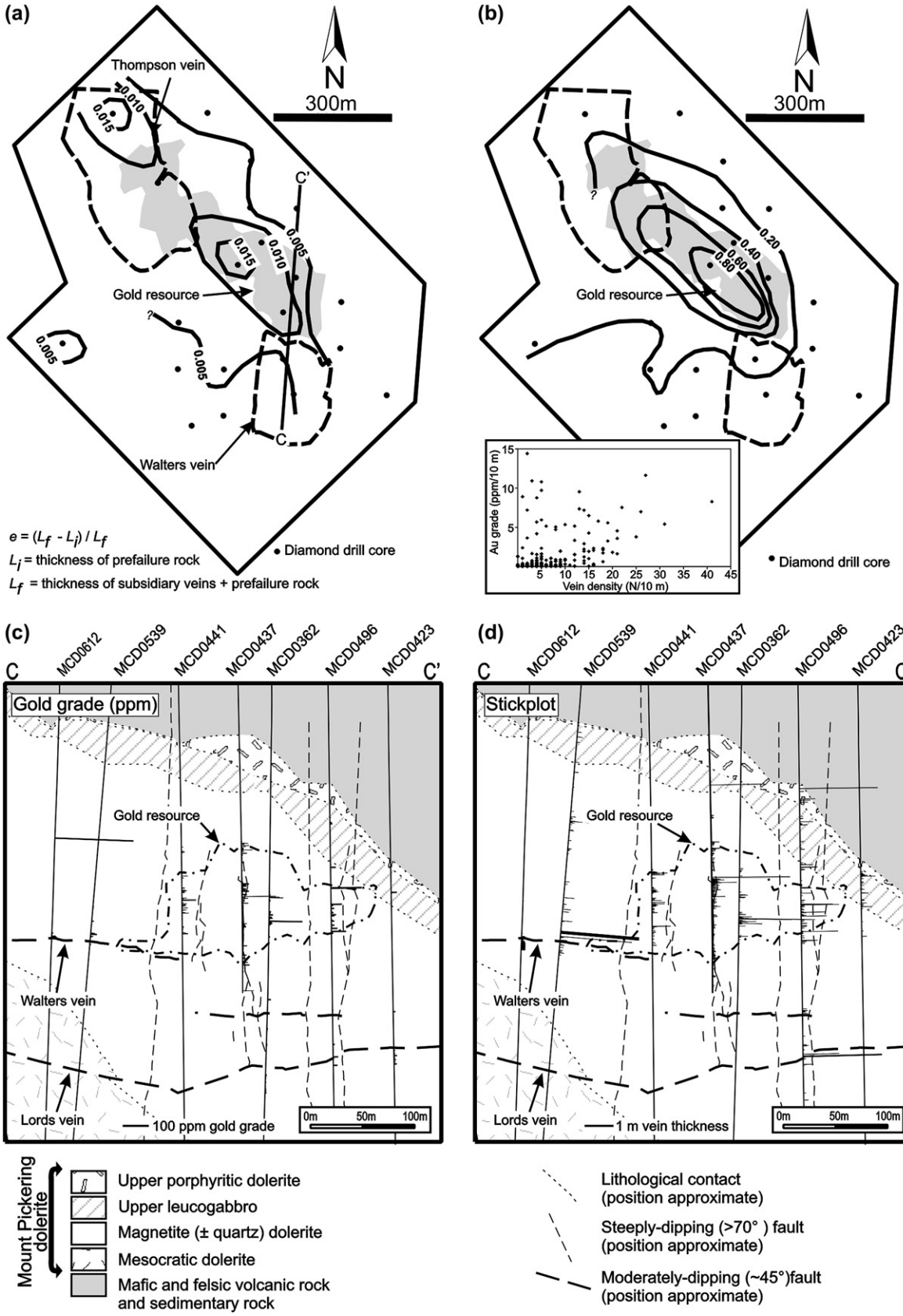

Fig. 17. Plans and sections showing the Centenary gold resource relative to distributions of bulk vertical extensional strain (e), vein density, and stickplots. Thick borders on diagrams in parts (a) and (b) correspond with area marked on Fig. 2. (a) Plan projection of the Centenary gold resource compared to bulk vertical extensional strain (e) for subsidiary veins. (b) Plan projection of the Centenary gold resource compared to vein density. Inset shows vein density versus gold grade calculated over 10 m intervals for the examined drill cores. (c) Gold grade in drill cores in a north-south section parallel to the Walters fault and across the zone of high bulk vertical extensional strain (e). The Centenary gold resource is shown. For location of section see Fig. 16. (d) North-south section parallel to the Walters fault and across the zone of high bulk vertical extensional strain (e) showing the distribution of veins and vein thickness compared to the Centenary gold resource. For location of section see Fig. 16.

Acknowledgements

This work forms part of a PhD study by SK who acknowledges receipt of an Australian Postgraduate Scholarship. The project is supported by Barrick Gold of Australia. Maptek provided Vulcan software used for three-dimensional modelling of structures and creation of sections. Dave Brookes and Liz Smith provided advice and guidance in the use of GIS software. Francois Robert, Trevor Beardsmore and Chris Black are thanked for useful discussions on the geology of the Darlot gold deposit. Darlot gold mine staff provided mine site support particularly Richard Hay, Lachie Reid, Dave Ford, John Slinger, Selwyn Jones, Wayne Zarb, Mike Stone, Kellie Paterson, Mike Falconer, Kym Wellstead, Ian Primmer and Wayne Harvey. An early version of the manuscript benefited from reviews by Trevor Beardsmore, Myra Keep and Klaus Gessner. Later versions of the manuscript benefited from detailed reviews by Paul Gillespie, Steve Cox, Richard Goldfarb, John Ridley and an anonymous reviewer. Fig. 4 was compiled from mapping by SK and geologists Dave Ford and John Slinger.

References

Barquins, M., Petit, J.P., 1992. Kinetic instabilities during the propagation of a branch crack: effects of loading conditions and internal pressure. Journal of Structural Geology 14, 893–903.

Beardsmore, T.J., Gardner, Y., 2003. Darlot gold deposit, Yandal gold province, Yilgarn Craton, Western Australia. In: Ely, K.S., Phillips, G.N. (Eds.), Yandal Gold Province: Geoscience and Exploration Success. CSIRO Exploration and Mining, pp. 173–219.

Bruhn, R.L., Yonkee, W.A., Parry, W.T., 1990. Structural and fluid-chemical properties of seismogenic normal faults. Tectonophysics 175, 139–157.

Chen, S.F., Witt, W.K., Liu, S., 2001. Transpression and restraining jogs in the northeastern Yilgarn Craton, Western Australia. Precambrian Research 106, 309–328.

Chester, F.M., Logan, J.M., 1986. Implications for mechanical properties of brittle faults from observations of the Punchbowl Fault Zone, California. Pure and Applied Geophysics 124, 79–106.

Chester, F.M., Evans, J.P., Biegel, R.L., 1993. Internal structure and weakening mechanisms of the San Andreas Fault. Journal of Geophysical Research 98, 771–786.

Cox, S.F., 1995. Faulting processes at high fluid pressures: an example of fault valve behavior from the Wattle Gully Fault, Victoria, Australia. Journal of Geophysical Research 100, 12841–12859.

Cox, S.F., Knackstedt, M.A., Braun, J., 2001. Principles of structural control on permeability and fluid flow in hydrothermal systems. In: Richards, J.P., Tosdal, R. (Eds.), Structural Controls in Ore Genesis. Reviews in Economic Geology, 14, pp. 1–24.

Evans, J.P., Forster, C.B., Goddard, J.V., 1997. Permeability of fault-related rocks, and implications for hydraulic structure of fault zones. Journal of Structural Geology 19, 1393–1404.

Foxford, K.A., Nicholson, R., Polya, D.A., Hebblethwaite, R.P.B., 2000. Extensional failure and hydraulic valving at Minas da Panasqueira, Portugal; evidence from vein spatial distributions, displacements and geometries. Journal of Structural Geology 22, 1065–1086.

Gardner, Y., Hagemann, S.G., Hay, R., 2001. Gold mineralization at the Darlot Centenary gold mine, southern Yandal greenstone belt, Eastern Goldfields Province, Western Australia: evidence for diverse mineralization styles and hydrothermal alteration types. In: Hagemann, S.G., Neumayr, P., Witt, W.K. (Eds.), World-class Gold Camps and Deposits in the Eastern Yilgarn Craton, Western Australia, with Special Emphasis on the Eastern Goldfields Province. Western Australia Geological Survey Record 2001/17, pp. 127–150.

Giles, C.W., 1982. The geology and geochemistry of the Archaean Spring Well felsic volcanic complex, Western Australia. Journal of the Geological Society of Australia 29, 205–220.

Gillerman, V.S., 1988. Comment and reply on "Earthquake rupturing as a mineralising agent in hydrothermal systems". Geology 16, 669–670.

Gillespie, P.A., Johnston, J.D., Loriga, M.A., McCaffrey, K.J.W., Walsh, J.J., Watterson, J., 1999. Influence of layering on vein systematics in line samples. In: McCaffrey, K.J.W., Lonergan, L., Wilkinson, J.J. (Eds.), Fractures, Fluid Flow and Mineralization. Geological Society, London, pp. 35–56 (Special Publications vol. 155).

Groves, D.I., Ridley, J.R., Bloem, E.M.J., Gebre-Mariam, M., Hagemann, S.G., Hronsky, J.M.A., Knight, J.T., McNaughton, N.J., Ojala, J., Vielreicher, R.M., McCuaig, T.C., Holyland, P.W., 1995. Lode-gold deposits of the Yilgarn block: products of Late Archaean crustal-scale overpressured hydrothermal systems. Early Precambrian Processes 95, 155–172.

Hagemann, S.G., Cassidy, K.F., 2000. Archean orogenic lode gold deposits. In: Hagemann, S.G., Brown, P.E. (Eds.), Gold in 2000. Reviews in Economic Geology, 13, pp. 9–68.

Harris, R.A., Day, S.M., 1993. Dynamics of fault interaction: parallel strike-slip faults. Journal of Geophysical Research 98, 4461–4472.

Kennworthy, S., Hagemann, S.G., Chanter, S.C., 2001. Structural control and mineralization style of the quartz-reef hosted Golden Age gold mine, Wiluna greenstone belt, Yilgarn Craton. In: Hagemann, S.G., Neumayr, P., Witt, W.K. (Eds.), World-class Gold Camps and Deposits in the Eastern Yilgarn Craton, Western Australia, with Special Emphasis on the Eastern Goldfields Province. Western Australia Geological Survey Record 2001/17, pp. 177–196.

Kim, Y.S., Peacock, D.C.P., Sanderson, D.J., 2003. Mesoscale strike-slip faults and damage zones at Marsalforn, Gozo Island, Malta. Journal of Structural Geology 25, 793–812.

Kim, Y.S., Peacock, D.C.P., Sanderson, D.J., 2004. Fault damage zones. Journal of Structural Geology 26, 503–517.

Kohler, E.A., Phillips, G.N., 2003. Jundee goldfield, Yandal gold province, Yilgarn Craton, Western Australia. In: Ely, K.S., Phillips, G.N. (Eds.), Yandal Gold Province: Geoscience and Exploration Success. CSIRO Exploration and Mining, pp. 81–132.

Kohler, E.A., Davies, B., Phillips, G.N., Vearncombe, J.R., Mason, R., Chanter, S., 2003. Bronzewing gold deposit, Yandal gold province, Yilgarn Craton, Western Australia. In: Ely, K.S., Phillips, G.N. (Eds.), Yandal Gold Province: Geoscience and Exploration Success. CSIRO Exploration and Mining, pp. 139–172.

Krcmarov, R.L., Beardsmore, T.J., King, J., Kellett, R., Hay, R., 2000. Geology, regolith, mineralization and mining of the Darlot-Centenary gold deposit, Yandal belt. In: Phillips, G.N., Anand, R.R. (Eds.), Yandal Greenstone Belt. Australian Institute of Geoscientists Bulletin, 32, pp. 351–372.

McGrath, A.G., Davison, I., 1995. Damage zone geometry around fault tips. Journal of Structural Geology 17, 1011–1024.

Messenger, P.R., 2000. Geochemistry of the Yandal belt metavolcanic rocks, Eastern Goldfields Province, Western Australia. Australian Journal of Earth Sciences 47, 1015–1028.

Peltzer, G., Rosen, P., Rogez, F., Hudnut, K., 1996. Postseismic rebound in fault step-overs caused by pore fluid flow. Science 273, 1202–1204.

Phillips, G.N., Vearncombe, J.R., 2003. Exploration of the Yandal gold province, Yilgarn Craton, Western Australia. In: Ely, K.S., Phillips, G.N. (Eds.), Yandal Gold Province: Geoscience and Exploration Success. CSIRO Exploration and Mining, pp. 1–26.

Phillips, G.N., Vearncombe, J.R., Eshuys, E., 1998. Yandal greenstone belt, Western Australia: 12 million ounces of gold in the 1990s. Mineralium Deposita 33, 310–316.

Ragan, D.M., 1985. Structural Geology: An Introduction to Geometrical Techniques. John Wiley and Sons, New York.

Rispoli, R., 1981. The stress fields about strike-slip faults inferred from styolites and tension gashes. Tectonophysics 75, 29–36.

Robert, F., Boullier, A.M., Firdaous, K., 1995. Gold-quartz veins in metamorphic terranes and their bearing on the role of fluids in faulting. Journal of Geophysical Research 100, 12861–12879.

Sanderson, D.J., Roberts, S., 1994. A fractal relationship between vein thickness and gold grade in drill core from La Codosera, Spain. Economic Geology 89, 168–173.

Segall, P., Pollard, D.D., 1980. Mechanics of discontinuous faults. Journal of Geophysical Research 85, 4337–4350.

Sibson, R.H., 1985. Stopping of earthquake ruptures at dilational fault jogs. Nature 316, 248–251.

Sibson, R.H., 2004. Controls on maximum fluid overpressure defining conditions for mesozonal mineralisation. Journal of Structural Geology 26, 1127–1136.

Sibson, R.H., Scott, J., 1998. Stress / fault controls on the containment and release of overpressured fluids: examples from gold-quartz vein systems in Juneau, Alaska; Victoria, Australia and Otago, New Zealand. Ore Geology Reviews 13, 293–306.

Sibson, R.H., Robert, F., Poulsen, K.H., 1988. High-angle reverse faults, fluid pressure cycling and mesothermal gold-quartz deposits. Geology 16, 551–555.

Travis, G.A., Woodall, R., Bartram, G.D., 1971. The geology of the Kalgoorlie goldfield. Special Publication Geological Society of Australia 3, 175–190.

Vearncombe, J.R., 1998. Shear zones, fault networks and Archaean gold. Geology 26, 855–858.

Westaway, J.M., Wyche, S., 1998. Geology of the Darlot 1:100,000 Sheet. Geological Survey of Western Australia, 1:100,000 Geological Series Explanatory Notes, 24.

Zhang, X., Sanderson, D.J., 1996. Numerical modelling of the effects of fault slip on fluid flow and extensional faults. Journal of Structural Geology 18, 109–119.